



SLOW SLIP EVENTS AND SEISMIC TREMOR AT CIRCUM-PACIFIC SUBDUCTION ZONES

Susan Y. Schwartz¹ and Juliana M. Rokosky¹

Received 22 June 2006; revised 5 January 2007; accepted 6 March 2007; published 22 August 2007.

[1] It has been known for a long time that slip accompanying earthquakes accounts for only a fraction of plate tectonic displacements. However, only recently has a fuller spectrum of strain release processes, including normal, slow, and silent earthquakes (or slow slip events) and continuous and episodic slip, been observed and generated by numerical simulations of the earthquake cycle. Despite a profusion of observations and modeling studies the physical mechanism of slow slip events remains elusive. The concurrence of seismic tremor with slow slip episodes in Cascadia and southwestern Japan provides insight into the process of slow slip. A perceived similarity between subduction zone and volcanic tremor has led to suggestions that slow slip involves fluid migration on or near the plate interface. Alternatively, evidence is accumulating to support the notion that tremor results from shear failure during slow slip. Global observations of the location, spatial extent, magnitude, duration, slip rate, and periodicity of these aseismic slip transients indicate significant variation that may be exploited to better understand their generation. Most slow slip events occur just downdip of the seismogenic zone,

consistent with rate- and state-dependent frictional modeling that requires unstable to stable transitional properties for slow slip generation. At a few convergent margins the occurrence of slow slip events within the seismogenic zone makes it highly likely that transitions in frictional properties exist there and are the loci of slow slip nucleation. Slow slip events perturb the surrounding stress field and may either increase or relieve stress on a fault, bringing it closer to or farther from earthquake failure, respectively. This paper presents a review of slow slip events and related seismic tremor observed at plate boundaries worldwide, with a focus on circum-Pacific subduction zones. Trends in global observations of slow slip events suggest that (1) slow slip is a common phenomena observed at almost all subduction zones with instrumentation capable of recording it, (2) different frictional properties likely control fast versus slow slip, (3) the depth range of slow slip may be related to the thermal properties of the plate interface, and (4) the equivalent seismic moment of slow slip events is proportional to their duration ($M_o \propto \tau$), different from the $M_o \propto \tau^3$ scaling observed for earthquakes.

Citation: Schwartz, S. Y., and J. M. Rokosky (2007), Slow slip events and seismic tremor at circum-pacific subduction zones, *Rev. Geophys.*, 45, RG3004, doi:10.1029/2006RG000208.

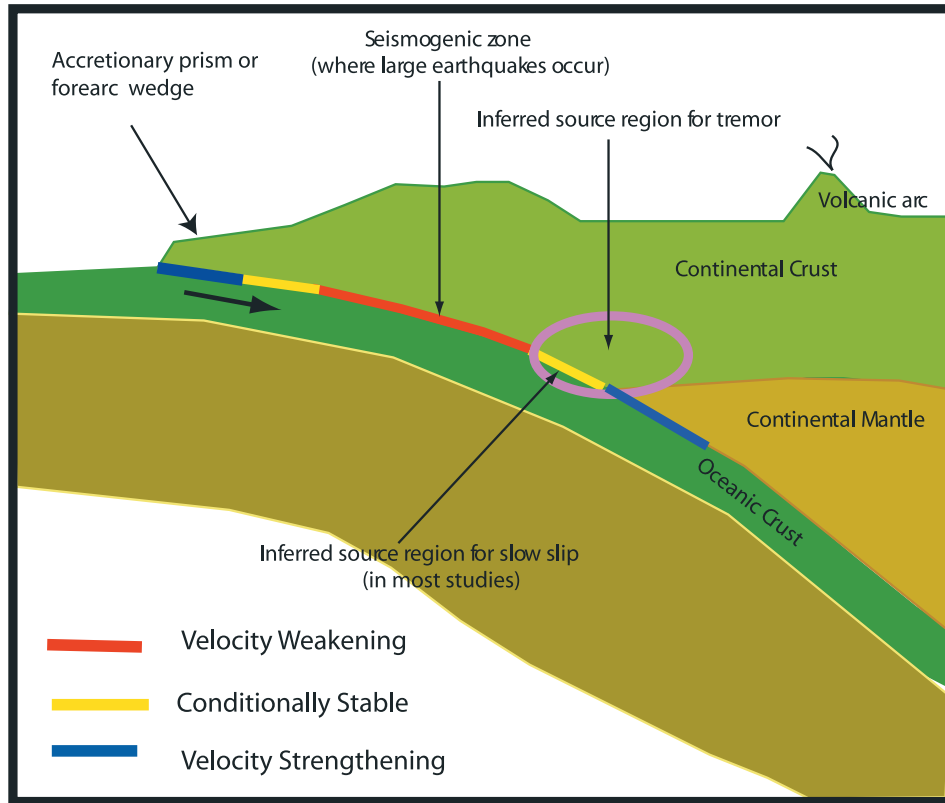
1. INTRODUCTION TO STRAIN RELEASE AT PLATE BOUNDARIES

[2] Most plate boundaries accommodate far-field motions on localized zones of deformation through aseismic creep at depth and earthquake failure in the upper crust. Earthquake slip and transition with depth from seismic to aseismic deformation can be understood in terms of the frictional response of materials. Realistic faults have a complicated dependence of friction on slip velocity, time, and slip distance (known as rate- and state-dependent friction). If frictional resistance to fault movement decreases faster than stress reduces due to movement, sliding may occur in sudden slips with associated stress drops (earthquakes), punctuated by periods of no motion as stress recharges. This motion is commonly referred to as stick

slip, and the frictional behavior is referred to as velocity weakening. If this condition is not met and fault strength does not decrease with slip, stable sliding will occur. The frictional behavior of stable sliding is known as velocity strengthening. As temperature increases with depth, a transition from velocity weakening to velocity strengthening frictional behavior is believed to be responsible for the termination of earthquakes and accommodation of plate motion through stable sliding. The region of the plate boundary exhibiting velocity weakening behavior and capable of generating earthquakes is often referred to as the seismogenic zone (Figure 1a). The seismogenic zone possesses a second frictional transition to velocity strengthening (stable sliding) at its shallow updip edge. Although earthquakes do not nucleate outside of the seismogenic zone, seismic rupture propagation has been observed to extend into both the updip and downdip stable sliding frictional regimes. The frictional property of these regions of the fault that can propagate but not nucleate seismic rupture is known as conditional stability.

¹Department of Earth and Planetary Sciences and Institute of Geophysics and Planetary Physics, University of California, Santa Cruz, California, USA.

a)



b)

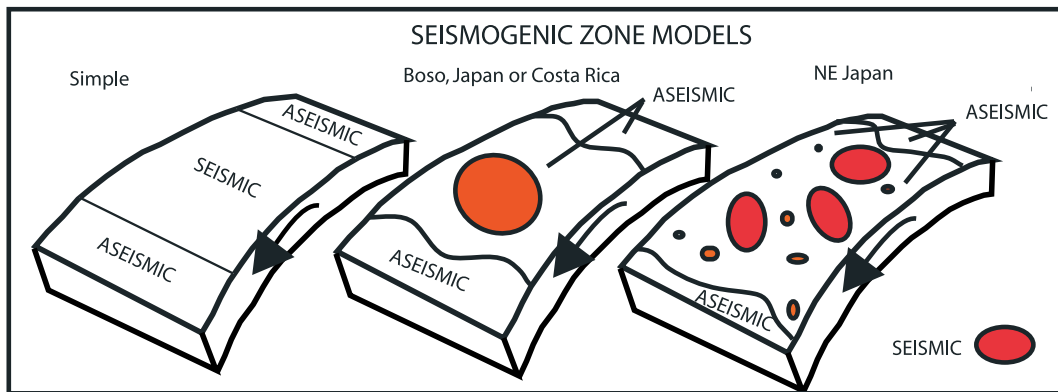


Figure 1. (a) Schematic of the seismogenic zone at convergent plate boundaries with frictional properties labeled. Earthquakes nucleate in velocity weakening materials and are capable of propagating into conditionally stable but not velocity strengthening regions. (b) Cartoons of the plate interface at different types of convergent margin seismogenic zones. The simple model contains only two frictional transitions from velocity weakening (seismic) to conditionally stable or velocity strengthening (aseismic) behavior at its updip and downdip limits. The Boso or Costa Rica model (middle) and northeast Japan model (right) have these transitions within the seismogenic zone. Slow slip events (SSEs) nucleate at these frictional transitions with most occurring at the deeper transition. The extreme frictional heterogeneity of the northeast Japan subduction zone may prevent SSEs from initiating within its seismogenic zone.

[3] On timescales of years, strain accumulates at plate boundary seismogenic zones as stress from plate motions builds. When the stress reaches a failure threshold, strain release occurs via large earthquakes. However, several

continental strike-slip faults, such as the San Andreas Fault, exhibit segments that release strain fairly continuously or creep both at the surface [Galehouse, 2002] and at seismogenic depths [Wesson, 1988]. Creeping segments were first

recognized by offsets of cultural features and an abundance of microseismicity in the absence of sizable earthquakes. Although the microseismicity may occur at a high rate, it does not contribute significantly to total fault slip, and the majority of the accumulating strain in these fault segments is released through aseismic creep. The microseismicity associated with creeping faults has been interpreted as small patches of velocity weakening material embedded within primarily velocity strengthening material, complicating the relatively simple picture of the seismogenic zone shown in Figure 1. Slip at depth on some segments of the surface creeping Hayward Fault in California has been quantified through the inversion of geodetic data [Bürgmann *et al.*, 2000; Simpson *et al.*, 2001; Malservisi *et al.*, 2003] and reveals that the fault zone consists of a patchwork of frictional properties with behaviors ranging from completely locked patches (no observable slip) to continuously slipping zones (moving at the surface velocity). Mid-ocean ridge transform faults have also been shown to accommodate much of their plate motions (up to 85%) aseismically [Boettcher and Jordan, 2004].

[4] Although much less is known about aseismic slip in the seismogenic zones of subduction faults, recent work at convergent margins in northeast and southwest Japan revealed a patchwork of seismically and aseismically slipping regions similar to the Hayward Fault [e.g., Igarashi *et al.*, 2003]. Figure 1b shows schematic representations of the surface of the seismogenic zone of subduction thrust faults. The cartoon on the far left indicates the updip and downdip frictional transitions from velocity weakening (seismic) to velocity strengthening (aseismic) with no variations in frictional properties within each region. For the other cartoons, seismic/aseismic frictional transitions exist within as well as at the updip and downdip edges of the seismogenic zone. Accumulating knowledge from seismic, geodetic, and modeling studies of the plate interface at convergent margins seems to favor the more complicated models.

[5] Slip rates during earthquakes can be on the order of meters per second, while creep rates are closer to plate motion velocities of millimeters per year, as much as 10 orders of magnitude slower. Slip occurring at intermediate timescales has been reported from both direct and indirect observations. The existence of slow earthquakes was postulated on the basis of analysis of anomalous free oscillations of the Earth [Beroza and Jordan, 1990], weak seismic radiation at high frequencies or anomalous low-frequency radiation [Newman and Okal, 1998; Kanamori and Stewart, 1976; Pérez-Campos *et al.*, 2003], or strong tsunami relative to seismic excitation [Pelayo and Wiens, 1992]. Some examples of slow earthquakes include a predecessor to the great 1960 Chilean earthquake [Kanamori and Cipar, 1974; Linde and Silver, 1989], a successor to the 1978 Izu-Oshima, Japan, earthquake [Sacks *et al.*, 1981], and the 1992 Nicaragua tsunami earthquake [Kanamori and Kikuchi, 1993]. We term these and other events that have slow source processes but still radiate seismic energy “slow earthquakes.” The relative slowness of these events has been attributed to unusual material properties along the fault interface [e.g., Bilek *et*

al., 2004] such that a large amount of energy is dissipated during deformation, making less energy available for seismic radiation. The existence of events having much longer source durations of days to years was first postulated for a segment of the San Andreas Fault on the basis of borehole strainmeter data [Linde *et al.*, 1996]. Unlike the slow earthquakes described above the slip during this event occurred over hours to days, too slow to generate seismic radiation. This slow duration is more likely associated with the time for slip on the fault to reach its final value (slip risetime) rather than a rupture propagation time. We will refer to this and other slip episodes initiating in or near the seismogenic zone but radiating no seismic energy as “slow slip events” (SSEs). Although other researchers have used the terms “slow” or “silent earthquakes,” “aseismic strain transients,” or “creep events” to describe this phenomenon, we have discovered no consistent and uniformly applied nomenclature in the literature to describe slip events with the large range of slip durations observed.

[6] Continuous Global Positioning System (GPS) networks have enabled the recording of this important class of geophysical phenomena, and recently, slow slip has been detected with continuous GPS networks in Japan [Heki *et al.*, 1997; Hirose *et al.*, 1999; Ozawa *et al.*, 2001], Cascadia [Dragert *et al.*, 2001], Mexico [Lowry *et al.*, 2001], Kamchatka [Bürgmann *et al.*, 2001], Alaska [Freymueller *et al.*, 2002], New Zealand [Douglas *et al.*, 2005], and Hawaii [Cervelli *et al.*, 2002]. These observations are allowing a much more complete understanding of strain accumulation and release at plate boundaries. The evolving picture is quite complex, with the rate of fault loading and unloading varying in both space and time. The full spectrum of strain release modes including dynamic instability (an earthquake), slow slip events, and continuous stable sliding is being captured with modern instrumentation and successfully modeled using rate- and state-dependent friction laws. The rapidly expanding number of continuous GPS observations of slow slip events is helping to constrain the mechanical properties at the plate boundaries where they occur. Seismic moment at most plate boundaries accounts for only a fraction of plate tectonic motions, so the inclusion of slow slip events can provide a better quantification of the moment release budget. Earthquake slip on one fault segment changes the stress on adjacent segments and may accelerate or decelerate seismic activity. This abrupt stress change may also initiate other modes of strain release, such as slow slip events. Conversely, slow fault slip also perturbs the surrounding stress field and may either increase or relieve stress on an adjacent fault segment, bringing it closer to or farther from earthquake failure, respectively. Therefore an improved understanding of slow slip events and their ability to trigger earthquakes is important for seismic hazard assessment.

2. SLOW SLIP EVENTS

2.1. Slow Slip Events and the Seismic Cycle

[7] On the basis of observations to date from around the globe several kinds of slow slip events have been recognized,

each having important implications for the seismic process. Since this review concentrates on slow slip events occurring at subduction zones, we can naturally categorize these events on the basis of when they occur in the seismic cycle. Slow slip that follows or precedes large earthquakes will be termed afterslip and preslip, respectively, and slow slip that occurs between large earthquakes will be called interseismic slip.

2.1.1. Afterslip

[8] Slow slip following moderate to large earthquakes, or afterslip, was first documented for the 1966 Parkfield earthquake along the San Andreas Fault [Smith and Wylss, 1968]. Since then it has been detected at many other strike-slip [Williams and Magistrale, 1989; Bucknam et al., 1978] and subduction zone thrust faults. We consider the following characteristics to be diagnostic of afterslip: (1) location on the coseismic fault plane, (2) slip duration of days to months with a rapid initial rate of slip followed by a logarithmic decay, and (3) cumulative values that approach or exceed 50% of the average coseismic slip. These distinguish afterslip from postseismic, viscoelastic relaxation where slip is typically distributed deeper in the lower crust and upper mantle and occurs over much longer timescales of years to tens of years and follows an exponential decay. It should be noted that with only limited observations of the surface deformation field, afterslip and viscoelastic relaxation cannot be uniquely distinguished. However, Hearn [2003] confirmed that surface displacement observations obtained from a well-distributed network of continuous or frequently occupied campaign mode GPS sites are sufficient to distinguish linear viscoelastic relaxation from afterslip. All slow deformation attributed to afterslip on coseismic fault planes reported in this paper has been so identified in the abovementioned studies.

[9] Marone et al. [1991] proposed a model for earthquake afterslip where the fault kinematics were prescribed by rate- and state-dependent friction laws. In this schema, unrelieved stresses on the fault induce aseismic slip after the earthquake within velocity strengthening regions of the fault. Their particular model consisted of a thin layer with velocity strengthening properties, such as fault gouge, overlying a much thicker velocity weakening layer. Coseismic rupture initiated and propagated in the lower layer but was arrested by the shallow velocity strengthening layer, which resulted in a stress concentration at the frictional transition that drove afterslip in the shallow layer. The existence of a slip deficit at shallow depth was required to drive the afterslip. Therefore, in their model, if coseismic rupture propagated to the surface, relaxing stress in the velocity strengthening layer, no afterslip was predicted. In fact, such a phenomenon was observed for the 1992 Landers, California, earthquake where significant coseismic slip extended to the surface [Wald and Heaton, 1994] and negligible afterslip was detected [Sylvester, 1993]. Marone et al.'s [1991] model is very well suited to vertical strike-slip faults that develop thick velocity strengthening gouge layers as they mature. It has successfully reproduced the afterslip time histories for the 1966 Parkfield and 1987

Superstition Hills, California, earthquakes and yielded estimates of the frictional transition depths and other important rheological properties of these fault zones from the logarithmic decay of the afterslip [Marone et al., 1991].

[10] With the increase in GPS monitoring of plate boundaries, numerous observations of afterslip have been made at shallow subduction zone thrust faults [Pritchard and Simons, 2006, Table 1]. For example, Hutton et al. [2001] reported measurable motion 3.5 years after the $M_w = 8.0$ 1995 Colima-Jalisco, Mexico, earthquake. While coseismic slip, of up to 5 m, was constrained to occur at depths between 0 and 20 km, afterslip amounting to as much as $\sim 70\%$ of coseismic motions occurred primarily downdip at depths between 16 and 35 km. Melbourne et al. [2002] documented moment of $\sim 25\%$ of the coseismic value occurring as afterslip, downdip from the main rupture within a few weeks of the $M_w = 8.4$ 2001 Peru earthquake. However, they found no significant afterslip, at a single continuous GPS station, following the $M_w = 8.1$ 1995 Antofagasta, Chile, event. Subsequently, Pritchard and Simons [2006] inverted interferometric synthetic aperture radar (InSAR) and GPS observations spanning 5 years following the Antofagasta earthquake and located afterslip totaling less than 20% of the coseismic slip, at the downdip edge of the seismogenic zone, in areas distinct from regions of maximum coseismic slip. The cumulative moment from afterslip approached or exceeded that released in the main shock for the $M_w = 7.7$ 1994 Sanriku-oki, Japan [Heki et al., 1997; Yagi et al., 2003], and the $M_w = 7.8$ 1997 Kamchatka earthquakes [Bürgmann et al., 2001]. In both cases, afterslip located downdip of the main shock slip concentrations or asperities. Afterslip following large subduction zone thrust events has primarily been reported to occur at the downdip edge of the seismogenic zone. This is likely due to the location of most GPS stations on land, directly above the deep plate interface. These network configurations provide little resolution of postseismic deformation occurring offshore. An exception to this is GPS observations following the $M_w = 8.7$ 2005 Nias, Indonesia, earthquake, which were made close enough to the trench to allow resolution of shallow afterslip. Eleven months of afterslip, equivalent to an $M_w = 8.2$ earthquake, occurred both updip and downdip of the main shock asperity [Kreemer et al., 2006; Hsu et al., 2006]. Although substantial afterslip was detected following the $M_w = 9.2$ 2004 Sumatra-Andaman earthquake, the lack of near-field deformation data made determination of specific locations of afterslip difficult. The best assessments place afterslip at shallow depth, occurring close to or possibly overlapping regions of coseismic slip and with larger displacements occurring in the northern section of the rupture, where coseismic slip was relatively small [Subarya et al., 2006; Vigny et al., 2006]. Afterslip following the $M_w = 8.0$ 2003 Tokachi-oki earthquake occurred within the same depth range as the coseismic slip (within the seismogenic zone) but at unique positions along strike, adjacent to but not overlapping the main shock asperities [Matsubara et al., 2005]. In other words, afterslip appears to fill in regions of slip deficit left by main shocks as predicted

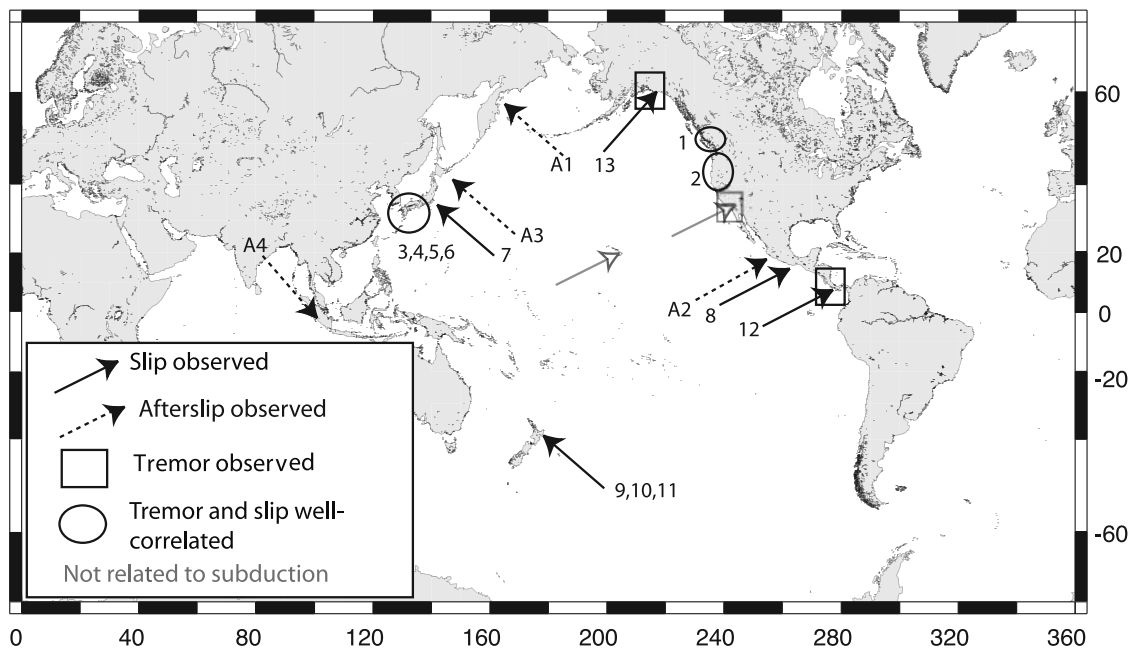


Figure 2. Map showing the location of slow slip events discussed in this review coded to represent interseismic slip (solid arrows), afterslip (dashed arrows), and slip not related to subduction (shaded arrows). The numbers correspond to those listed in Table 1. Circles and boxes represent regions where seismic tremor has been observed and is or is not well correlated with slow slip, respectively.

by state- and rate-dependent frictional models [Marone *et al.*, 1991].

[11] The locations and important details of some well-documented afterslip at subduction zones are indicated on Figure 2, listed in Table 1, and integrated with other observations of slow slip events occurring nearby in section 3.3. Afterslip is a particular class of slow slip events that is important to document and understand because it often accounts for as much slip as occurs in the main shock it follows. This large amount of afterslip may help explain the observation that seismic moment released at subduction plate boundaries is less than the total moment expected if all plate motion is accommodated seismically. Studies of afterslip are also important to test rate- and state-dependent friction laws. Accurate estimation of the decay time of afterslip as well as rigorous numerical tests of whether the observed decay is, in fact, logarithmic and remains so over the entire observing period will allow rate- and state-friction laws to be rigorously tested with field observations.

2.1.2. Preslip

[12] Anomalous, slow, aseismic motion immediately before great earthquakes has been reported in a few cases, for example, the $M_w = 7.9$ 1944 Tonankai and $M_w = 8.0$ 1946 Nankaido, Japan [Linde and Sacks, 2002, and references therein], and the $M_w = 9.5$ 1960 Chilean [Linde and Silver, 1989] subduction zone thrust earthquakes. For these great earthquakes, aseismic preslip was suggested in order to account for slow deformation detected on leveling, tide gauge, and water well level data, but details of the slow slip time histories were not determined. The relevant deformation data for the 1944 and 1946 events in southwest Japan were satisfied with 2 m of slow slip on the plate interface,

down dip of the coseismic slip. Preslip at the downdip extension of the seismogenic zone was also proposed for the smaller $M_w = 7.7$ 1983 Japan Sea thrust earthquake, on the basis of a borehole strainmeter recording of ~ 90 aseismic strain transient events [Linde *et al.*, 1988]. More recently, precursory slip before the largest aftershock of the $M_w = 8.4$ 2001 Peru earthquake was detected on a continuous GPS station in Arequipa, Peru, and shown to be consistent with slow slip along the plate interface [Melbourne and Webb, 2002].

[13] Roeloffs [2006] examined available data on aseismic deformation rate changes prior to earthquakes and reported 10 credible accounts of accelerated slip, lasting a few minutes to more than 10 years, preceding earthquakes ranging in magnitude between 3.5 and 9.2. Roeloffs [2006] also documented the absence of such anomalies for seven well-instrumented events with magnitudes between 6.0 and 8.4 and estimated the maximum equivalent preslip moment that may have been released and gone undetected by existing geodetic instrumentation. The paucity of positive preslip observations may in part be due to the existence of signals below the present detection thresholds. The expansion of continuous GPS networks, borehole strainmeters, and InSAR observations at plate boundaries should greatly improve the opportunity to detect and study preslip if and when it occurs.

2.1.3. Interseismic Slip

[14] Slow slip events occur on the subduction interface with no clear relation to major earthquakes and exhibit a large variation in duration, magnitude, and recurrence behavior. Dragert *et al.* [2001] documented an event in the northern Cascadia subduction zone with about 2 cm of

TABLE 1. Subduction Zone Slow Slip Event Characteristics^a

Geographic Region	Date, month/year	Slip, cm	M_w	τ , days	Recurrence, years	Migration, km/d	Tremor	References ^b
1, Northern Cascadia	9/1994	—	—	—	—	—	—	2
1, Northern Cascadia	12/1995	—	—	—	1.3	—	—	2
1, Northern Cascadia	5/1997	—	—	—	1.4	—	yes	2
1, Northern Cascadia	7/1998	3	6.8	—	1.2	10–20	yes	2
1, Northern Cascadia	8/1999	2–8	6.7–6.9	~50	1.1	6–15	yes	1, 2, 4
1, Northern Cascadia	12/2000	3	6.7	—	1.3	—	yes	2
1, Northern Cascadia	2/2002	4	6.5	—	1.2	—	yes	2
1, Northern Cascadia	3/2003	2–4	6.6	~40	1.1	5–10	yes	2, 5
1, Northern Cascadia	7/2004	3–4	6.8	~50	1.4	—	yes	2, 3
1, Northern Cascadia	9/2005	3–4	6.7	—	1.2	—	yes	6
2, Southern and central Cascadia ^c	—	—	—	—	—	—	—	7, 8
3, Bungo Channel - western Shikoku, SW Japan	—	—	—	—	—	—	—	—
Long term	3/1997	5–20	6.6–7.2	~300	—	yes	—	9, 11
Long term	8/2003	11	6.8–7.0	~90	6	yes	yes	10, 12
Short term ^d	8/2002	3.7	6.0	~5	0.5	yes	yes	13
Short term ^d	8/2003	3.9	6.1	~10	1	yes	yes	10
Short term ^d	11/2003	2.4	6.2	~7	0.25	yes	yes	10
Short term ^d	2/2004	2.1	6.0	~4	0.25	yes	yes	10
Short term ^d	4/2004	0.8	5.8	~5	0.17	yes	yes	10
4, Eastern Shikoku, SW Japan ^e	—	—	—	—	—	—	—	14
5, Kii Peninsula, SW Japan ^f	—	—	—	—	—	—	—	14, 15
6, Tokai, SW Japan	—	—	—	—	—	—	—	—
Long term	10/2000	20–30	>7.0	~2000	>10	yes	yes	16, 17, 18, 19, 20
Short term ^g	12/2004	1.8	5.8	4–5	~0.5	yes	yes	15
Short term ^g	7/2005	0.8	5.7	3	~0.5	yes	yes	15
7, Boso, central Japan	5/1996	~5	6.4–6.5	7	—	possible	no	22
	10/2002	~10–20	6.6	50	6	yes	no	21
8, Guerrero, Mexico ^h	10/2001	9–30	6.8–7.6	~200	<1	2	—	23, 24 and 25, 26, 27 ⁱ
9, Gisborne/Raukumara Peninsula, New Zealand ^j	10/2002	18	—	10	2–3	—	unclear	28, 29
	11/2004 ^k	—	—	—	—	—	—	28
10, Kapiti Coast, New Zealand	5/2003	50	—	~365	—	—	—	28
11, Manawatu region, New Zealand	1/2004	35	7.0	~549	—	updip, SW	—	28, 30
12, Costa Rica ^l	9/2003	1.5	—	30	—	downdip	—	31 and 32 ^m
13, Alaska-Aleutian subduction zone	1998	12–16	7.2	~1000	—	—	yes, unclear pattern	33, 34

Table 1. (continued)

Geographic Region	Date, month/year	Slip, cm	M_w	τ , days	Recurrence, years	Migration, km/d	Tremor	References ^b
Selected afterslip events								
A1, Kamchatka	12/1997	193	7.7	60	—	—	—	35
A2, Colima-Jalisco	10/1995	80	7.7	~150	—	down dip	—	36
A3, NE Japan	6/1978	100–200	7.5–7.6	1400	—	yes	—	40
A3, NE Japan	11/1989	—	7.4	10	—	—	—	38
A3, NE Japan	7/1992	>50	7.3–7.7	1	—	—	—	37, 38
A3, NE Japan	12/1994	120	7.5	100	—	—	—	38, 41
A3, NE Japan	8/2001	33	6.7	~65	—	—	—	39
A3, NE Japan	9/2003	40–60	7.8	~180	—	—	—	42
A4, Sumatra-Nias	12/2004	—	8.7	~45	—	—	—	45
A4, Sumatra-Nias	3/2005	50–140	8.2	~330	—	—	—	43, 44

^a M_w is equivalent moment magnitude; τ is event duration. Numbers in the first column correspond to Figure 2.

^bReferences are as follows: 1, *Dragert et al.* [2001]; 2, *Dragert et al.* [2004]; 3, *Gao and Schmidt* [2006]; 4, *McGuire and Segall* [2003]; 5, *Melbourne et al.* [2005]; 6, *Schmidt* [2006]; 7, *Bruzdinski and Allen* [2006]; 8, *Szeliga et al.* [2004]; 9, *Hirose et al.* [1999]; 10, *Hirose and Obara* [2005]; 11, *Miyazaki et al.* [2003]; 12, *Ozawa et al.* [2004]; 13, *Obara et al.* [2004]; 14, *Obara and Hirose* [2006]; 15, *Hirose and Obara* [2006]; 16, *Miyazaki et al.* [2006]; 17, *Ohta et al.* [2004]; 18, *Ozawa et al.* [2002]; 19, *Ozawa et al.* [2005]; 20, *Yamamoto et al.* [2005]; 21, *Ozawa et al.* [2003]; 22, *Sagiya* [2004]; 23, *Franco et al.* [2005]; 24, *Kostoglodov et al.* [2003]; 25, *Larson et al.* [2004]; 26, *Lowry et al.* [2001]; 27, *Lowry et al.* [2005]; 28, *Beavan et al.* [2007]; 29, *Douglas et al.* [2005]; 30, *Wallace and Beavan* [2006]; 31, *Protti et al.* [2004]; 32, *Brown et al.* [2005]; 33, *Ohta et al.* [2006]; 34, *Peterson et al.* [2005]; 35, *Bürgmann et al.* [2001]; 36, *Hutton et al.* [2001]; 37, *Kawasaki et al.* [1995]; 38, *Kawasaki et al.* [2004]; 40, *Ueda et al.* [2001]; 41, *Yagi et al.* [2003]; 42, *Matsubara et al.* [2005]; 43, *Hsu et al.* [2006]; 44, *Kreemer et al.* [2006]; 45, *Subarya et al.* [2006].

^cSeveral zones of periodic SSEs (identified from single GPS stations) that correlate with seismic tremor occur in this region. Recurrence intervals range between 11 and 19 months, and surface displacements are comparable to events in northern Cascadia.

^dThese events are identified by tilt changes approximately every 6 months from January 2001, lasting 5–7 days. Slip events are always accompanied by tremor, and slip and tremor migrate together.

^eEvents are identified by tilt changes in July 2001, November 2001, February 2002, May 2002, October 2002, and June 2003, each lasting several days to a week and strongly correlated with seismic tremor. Size of postulated SSEs is smaller than short-term events in western Shikoku.

^fEvents are identified by tilt changes in March 2001, September 2001, March 2002, October 2002, August 2003, January 2004, and November 2004, each lasting several days to a week and strongly correlated with seismic tremor. Size of postulated SSEs is smaller than short-term events in western Shikoku.

^gSlow slip with associated tremor is observed in Tokai with an approximately 6 month recurrence interval. Short-term SSEs appear to nucleate below the source area of the long-term Tokai SSE.

^hEvents are identified by campaign and continuous GPS and leveling observations in 1995–1996, 1999, 2000, early 2001, 2003, and 2004, with sizes that are slightly less than the October 2001 event and durations between 70 and 220 days. The apparent recurrence interval of SSEs in the region is ~1 year.

ⁱIn this row, references 23 and 24 refer to the date, and references 25, 26, and 27 refer to the geographic region.

^jThis event appears to have similar characteristics to October 2002 event.

^kSeveral small events are suggested from data at one GPS site to the south of these events, which may be related to Gisborne and Manawatu SSEs.

^lPostulated SSEs occur on February 2000, April 2000, and June 2000, recognized as correlated fluid flow, and seismic tremor episodes are measured on the ocean bottom lasting 2–3 weeks each [Brown et al., 2005].

^mIn this row, reference 31 refers to the date, and reference 32 refers to the geographic region.

slip that occurred on the plate interface over a period of several weeks (moment equivalent to a $M \sim 6.7$ earthquake) in a region where the last large interplate earthquake occurred over 300 years ago. More recent work revealed that northern Cascadia slow slip events locate downdip of the seismogenic zone near the seismic/aseismic transition, repeat at 13 to 16 month intervals, and are accompanied by seismic tremor [Miller *et al.*, 2002; Rogers and Dragert, 2003]. Ozawa *et al.* [2002] described a slow slip event on the subduction interface in the Tokai region of Japan that continued for over 4 years [Ohta *et al.*, 2004]. Similar events have been reported in southern Mexico [Lowry *et al.*, 2001], Alaska [Freymueller *et al.*, 2002], New Zealand [Douglas *et al.*, 2005], and Costa Rica [Protti *et al.*, 2004]. In fact, almost all subduction zones instrumented with a dense GPS network sufficient to detect SSEs have done so. One notable exception is the subduction zone off of northern Honshu, where a very dense GPS network has recorded several episodes of afterslip but no interseismic slow slip events. Like afterslip, most interseismic slow slip events have been reported to occur at the downdip extension of the seismogenic zone in the conditionally stable frictional regime. Because of the large range in behaviors exhibited by interseismic slow slip events, which may provide clues to their presently poorly understood generation, much of this review is devoted to them. Documenting the behavior of these events in all subduction zones and comparing and contrasting their behaviors may contribute to a better understanding of how and why they occur and whether they perturb the local stress field in a manner that brings the megathrust closer to failure in a great earthquake.

2.2. Slow Slip Events and Seismic Tremor

[15] Slow slip events release accumulated plate boundary strain with durations on the order of days to years. One of the important characteristics of these events is their inability to generate seismic radiation, and thus they have been referred to as “silent” earthquakes. Although extremely slow motion of faults generates no detectable seismic signal, Rogers and Dragert [2003] discovered that SSEs in northern Cascadia correlate with episodes of seismic tremor, a signal that is commonly associated with active volcanoes. Peaks in seismic tremor activity have also been robustly tied to SSEs in southwest Japan [Hirose and Obara, 2005]. Volcanic tremor was first reported from Aso Volcano in Japan in 1935 [Sassa, 1935] and has since been observed at hundreds of volcanoes worldwide. Volcanic tremor is a long-lasting vibration of the ground recorded by seismic instruments near volcanoes. It differs from tectonic earthquake recordings in its very long duration, lack of impulsive seismic arrivals, lower dominant frequencies, and often harmonic character (sharply peaked spectra with regular spacing). Several mechanisms for the generation of volcanic tremor have been proposed (from resonance of magma bodies of various geometries to unsteady fluid flow in constricted conduits). Although they differ widely, these mechanisms all share an association with the underground movement of fluids. As a result, the observation of similar

tremor behavior concurrent with SSEs was greeted with excitement because it bolstered models of slow slip that invoked the action of fluids.

[16] Slow slip events that exhibit correlated peaks in seismic tremor are noted in Figure 2 and Table 1. In section 3 we provide an overview of the general characteristics of seismic tremor associated with SSEs and more specific information about tremor observed at various locations worldwide. Tremor characteristics are summarized by location in Table 2.

3. GLOBAL OBSERVATIONS OF SLOW SLIP EVENTS AND SEISMIC TREMOR

3.1. General Characteristics of Slow Slip Events

[17] At a subduction zone where the plate interface is locked the downgoing slab drags the overlying plate with it in the direction of plate motion, producing a horizontal surface displacement field above the coupled plate boundary that parallels the convergence direction. This strain accumulation pattern develops during the interseismic phase of the earthquake cycle. When the strain reaches the failure strength of the fault, an earthquake occurs and sudden slip on the plate interface causes the upper plate to spring back to its former position. At the surface, displacement occurs in the opposite direction of strain accumulation, and this motion is complete within seconds to minutes, depending on the size of the earthquake. Following postseismic motions, the strain accumulation cycle begins again, and surface displacements return to paralleling the convergence direction. This strain accumulation and release pattern associated with the earthquake cycle is clearly visible in the daily position changes recorded at GPS station Arequipa (AREQ) in Peru above the South American subduction zone (Figure 3a). The linear northeast motion visible in the 500 days preceding the 2001 $M_w = 8.4$ Peru earthquake is parallel to convergence between the Nazca and South American plates and represents interseismic strain accumulation on the plate interface. On 23 June 2001 (day 0 in Figure 3a) a large displacement of 30–40 cm with the opposite sense of motion (southwest) indicates the sudden occurrence of slip on the plate interface, or an earthquake. This event was followed by afterslip for several months before the strain accumulation pattern resumed at the same rate as prior to the earthquake. Figure 3b shows a similar pattern in daily longitudinal position changes at GPS station ALBH on Vancouver Island, overlying the Cascadia subduction zone; however, here the earthquake-like motion that occurs on day 230 is much smaller (~ 5 mm) and takes almost 20 days to complete before returning to the strain accumulation signal. Surface velocities and displacements for the strain accumulation period (black vectors) and the slow slip event (red vectors) determined at GPS stations operated by the Geological Survey of Canada and part of the Pacific Northwest Geodetic Array are shown in Figure 3c. The slow earthquake-like motion, bracketed in time by strain accumulation signals (Figure 3b), is how slow slip events are identified from GPS time series. The iden-

TABLE 2. Seismic Tremor Characteristics

Kind of Tremor	Geographic Region	Dates Observed, month/year	Recurrence Interval	Episode Duration	Tremor Location	References ^a
Subduction zone tremor associated with SSEs	northern Cascadia	5/1997, 7/1998, 8/1999, 12/2000, 2/2002, 3/2003, 7/2004, and 9/2005	14 months	10–20 days	distributed in depth between ~10 and 40 km mostly in the overriding plate, above down-dip edge of the seismogenic zone	1, 2, 3, 4, 5, 6, 7
Subduction zone tremor associated with SSEs	southern and central Cascadia	1/2000 to present	various	up to 20 days	too few recordings to locate	6, 8, 9
Subduction zone tremor associated with SSEs	Bungo Channel–western Shikoku	1/2001 to present	6 months	several days to weeks	distributed along strike of subducting plate at 35–45 km depth (base of seismogenic zone).	10, 11, 12, 13, 15
Subduction zone tremor associated with SSEs	eastern Shikoku	1/2001 to present	~2–3 months	several days	appears to be similar to W. Shikoku	14
Subduction zone tremor associated with SSEs	Kii Peninsula	1/2001 to present	6 months	several days	appears to be similar to W. Shikoku	11, 14
Subduction zone tremor associated with SSEs	Tokai	2001 to present	6 months	several days	appears to be down-dip of source region of the long-term SSE	11, 16
Subduction zone tremor not clearly associated with SSEs	Nicoya Peninsula, Costa Rica	3 episodes between 1/2000 and 6/2000	unknown	up to 20 days	unknown, but correlated with anomalous fluid flow possibly caused by SSE	17
Subduction zone tremor not clearly associated with SSEs	Alaska-Aleutian subduction zone	intermittently during Alaska SSE	not reported	not reported	in region of 40–50 km contour of subducting plate	18
Subduction zone tremor triggered by distant earthquakes	Bungo Channel–western Shikoku	8/2003 and 12/2004	—	several thousand seconds	similar location as tremor associated with SSEs in this region	19, 20
Tremor at strike-slip fault	Cholame, California	12/2000–12/2003	—	0–5 episodes per day for 3 year period	below seismogenic zone at 20–40 km depth, along 25 km segment of the San Andreas Fault near Cholame, CA	21

^aReferences are as follows: 1, *Rogers and Dragert* [2003]; 2, *Dragert et al.* [2004]; 3, *Kao et al.* [2005]; 4, *Kao et al.* [2006]; 5, *La Rocca et al.* [2005]; 6, *McCausland et al.* [2005]; 7, *Royle et al.* [2006]; 8, *Szeliga et al.* [2004]; 9, *Brudzinski and Allen* [2006]; 10, *Obara* [2002]; 11, *Katsumata and Kamaya* [2003]; 12, *Obara et al.* [2004]; 13, *Hirose and Obara* [2005]; 14, *Obara and Hirose* [2006]; 15, *Shelly et al.* [2006]; 16, *Hirose and Obara* [2006]; 17, *Brown et al.* [2005]; 18, *Peterson et al.* [2005]; 19, *Miyazawa and Mori* [2005]; 20, *Miyazawa and Mori* [2006]; 21, *Nadeau and Dolenc* [2005].

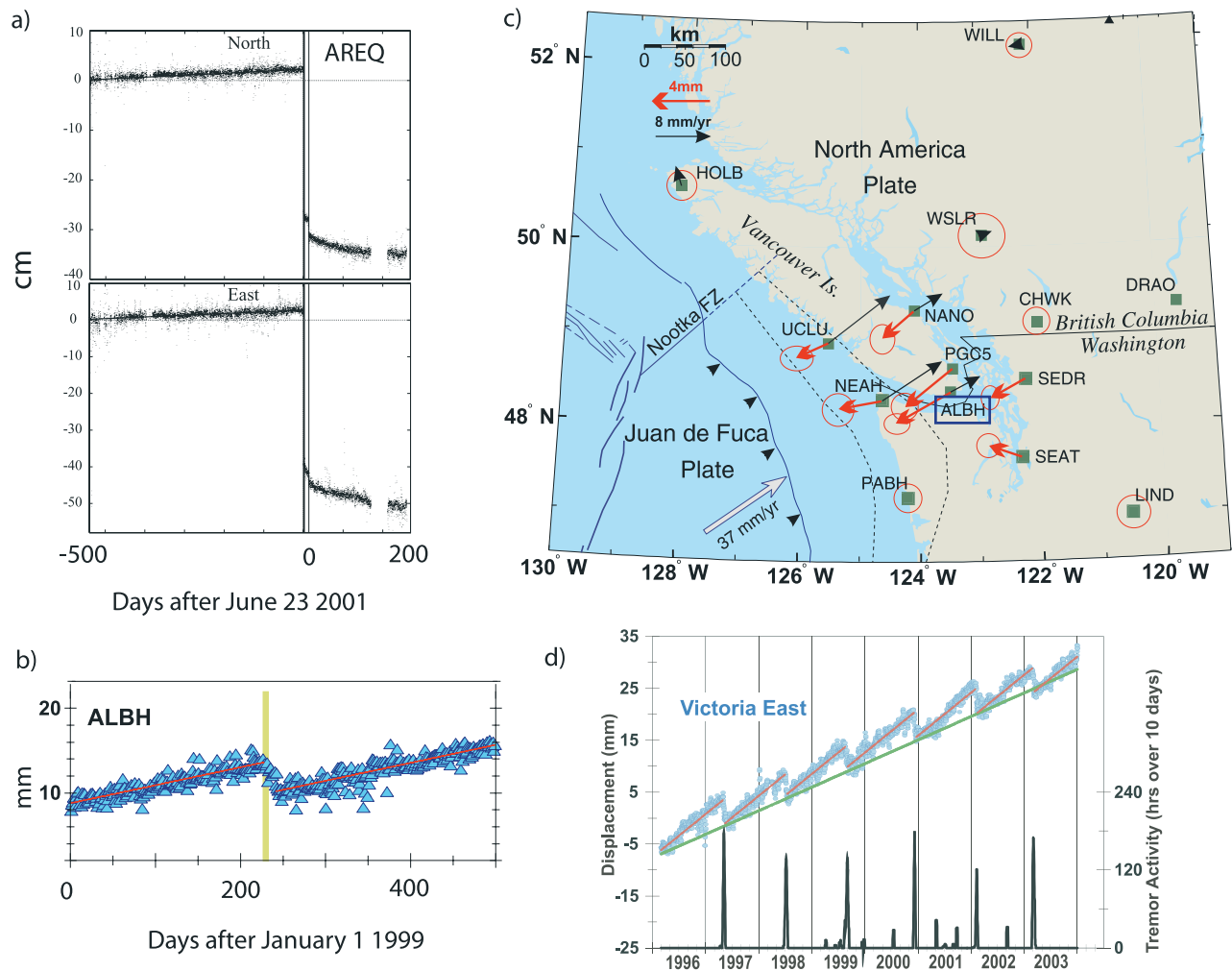


Figure 3. (a) Horizontal position solutions showing interseismic (slow linear northeast motion), coseismic (large, nearly instantaneous southwest motion), and postseismic deformation (slow southwest motion) recorded at GPS station AREQ before and after the 23 June 2001 $M_w = 8.4$ Peru earthquake, modified from *Melbourne and Webb* [2002]. (b) Longitudinal position solutions at GPS station ALBH, above the northern Cascadia subduction zone showing a slow slip event (marked by green line) that occurred in August 1999. Modified from *Dragert et al.* [2001], copyright Her Majesty the Queen in right of Canada (2001). (c) Map showing the location of the GPS stations that recorded the 1999 SSE. Red arrows show displacements caused by the SSE, and black arrows indicate the interseismic strain accumulation velocities. Modified from *Dragert et al.* [2001], copyright Her Majesty the Queen in right of Canada (2001). (d) Correlated slow slip and seismic tremor activity in the northern Cascadia subduction zone. Blue circles show east positions at GPS station ALBH, the green line indicates the long-term eastward strain accumulation signal, which is interrupted by SSEs (causing motion reversals) about every 13–16 months. Bottom graph shows the total number of hours of tremor observed over a 10 day period. Bursts in tremor activity strongly correlate with the SSEs. Modified from *Dragert et al.* [2004].

tification of SSEs in GPS displacement time series that may contain other deformation signals or be contaminated by meteorologic effects, local monument motion, and/or reference frame errors, is difficult and requires careful signal processing techniques [e.g., *McGuire and Segall*, 2003]. Once an SSE is identified, its surface displacement field can be modeled using elastic dislocation theory [*Okada*, 1985] to determine its location on an assumed fault plane, average slip (d) or slip rate, and seismic moment ($M_0 = \mu Ad$, where A is the fault area and μ is the shear modulus of the surrounding material) or equivalent earthquake moment-

magnitude ($M_w = 2/3 \log[M_0] - 6.07$, with M_0 in Nm). In regions such as Japan, with dense data coverage, surface displacements can be inverted for the nonuniform distribution of slip or slip rate as a function of time on the assumed fault plane. Similar to coseismic slip during earthquakes, slow slip has been shown to vary over the fault plane with isolated patches of higher or faster slip. Variations in the timing of anomalous surface displacements at GPS stations at different locations have been used to qualitatively assess slip migration patterns; however, when detailed slip distri-

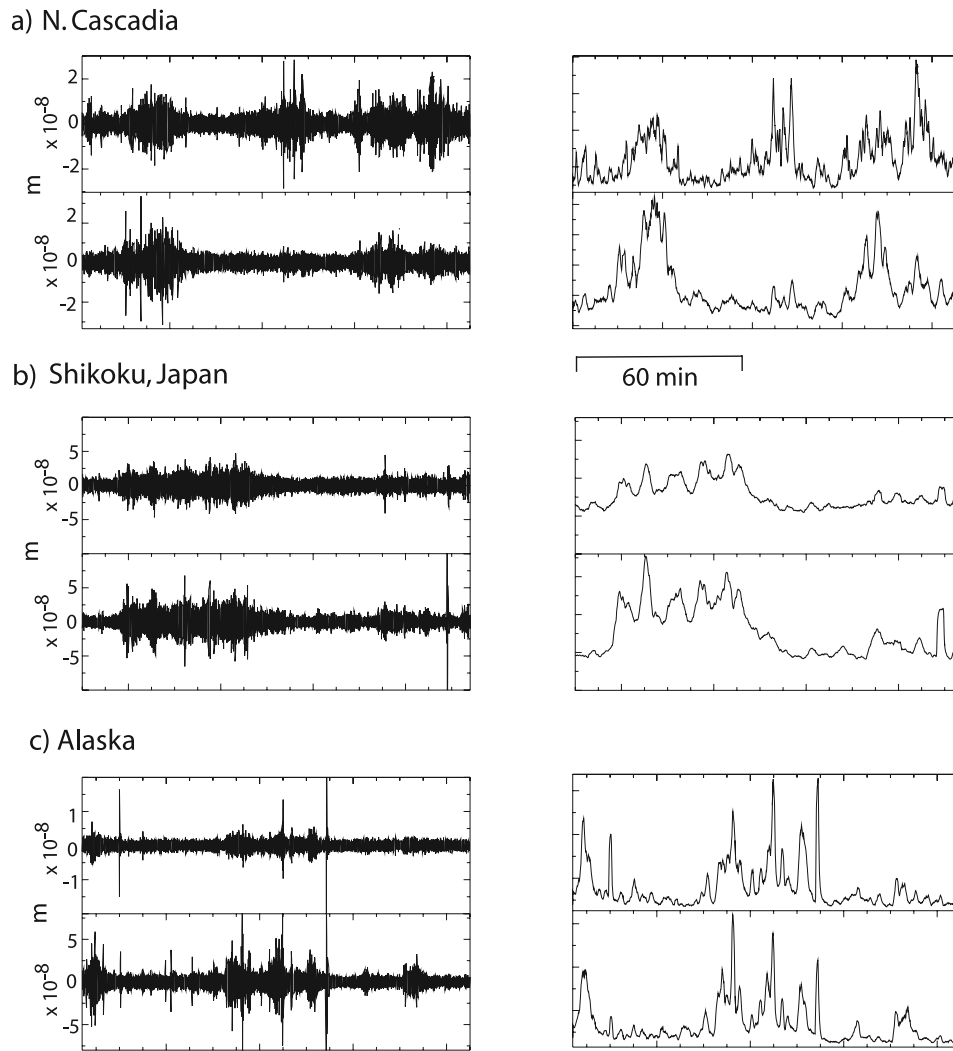


Figure 4. (left) Horizontal records of tremor from two stations in (a) northern Cascadia, (b) western Shikoku, Japan, and (c) southeastern Alaska. All records are 8400 s long and band-pass filtered between 2 and 4 Hz. Note that amplitude scales vary between records. (right) Envelope processed versions of the same records. These envelopes emphasize periods of tremor, which can be correlated between stations for identification and location.

butions are determined, migration patterns and rates for slow slip episodes can be more precisely calculated.

[18] Figure 2 shows the location of all well-documented SSEs from the literature discussed in section 3.3. Slow slip events are distributed globally and, in general, occur at nearly all plate boundaries that generate large earthquakes and have adequate instrumentation to detect them. These criteria are most commonly met at subduction zones, so it is not surprising that the majority of SSEs locate in this tectonic setting. Section 3.3 discusses relevant details of the SSEs observed in each geographic region, and Table 1 summarizes this information for subduction zone SSEs using the characteristics defined above. Those attributes of SSEs that are particularly important in evaluating candidate mechanisms and that will be highlighted in section 3.3 include (1) location on the fault plane relative to frictional stability transitions and main shock asperities, (2) size (M_o , M_w , and d), (3) event duration (τ), (4) repeatability and

recurrence interval, (5) migration patterns, and (6) association with seismic tremor.

3.2. General Characteristics of Seismic Tremor

[19] Tremor represents long duration (minutes to hours) of high-amplitude seismic signal, without clear body wave arrivals. Tremor duration varies between regions and episodes, and it is sometimes quite pulsed in nature (filtered waveforms are shown in Figure 4). Tremor is generally identified by the coincidence of high-amplitude envelopes on several nearby stations [e.g., Obara, 2002; McCausland *et al.*, 2005]. Figure 4 (right) shows envelope functions computed taking absolute values of the seismic records shown in Figure 4 (left). These envelopes show that increased amplitude of tremor can persist for over 30 min. The actual shape of these envelopes is correlated between different stations to identify tremor as a relatively widespread phenomenon, rather than a noise process isolated near a single station. Tremor activity has traditionally been

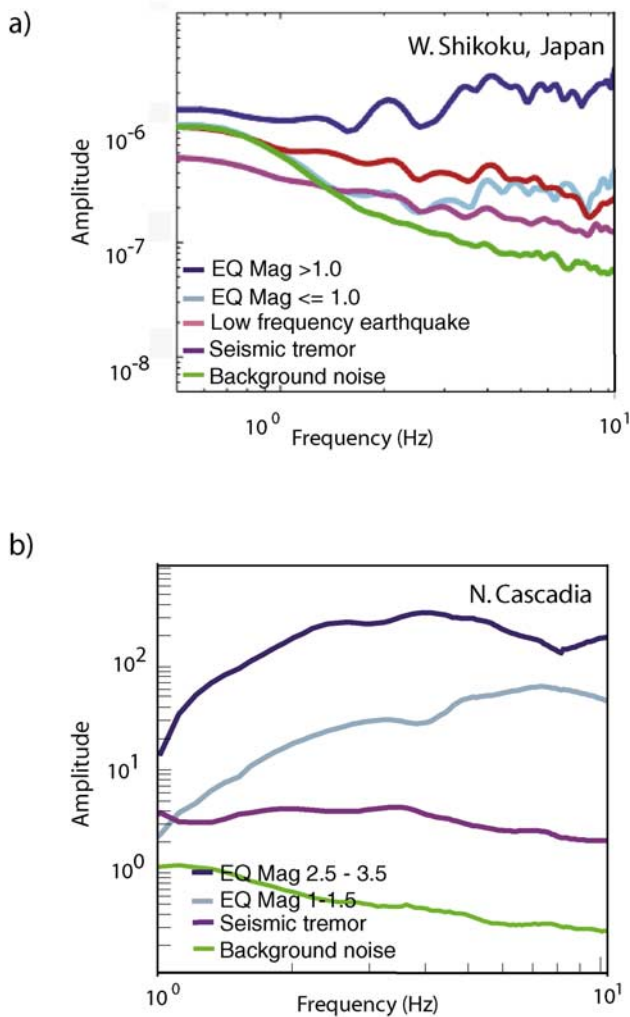


Figure 5. Comparison of stacked spectral amplitude from velocity seismograms from multiple nearby events of various kinds in (a) western Shikoku, Japan (provided by David Shelly), and (b) northern Cascadia (modified from Kao *et al.* [2006]). Amplitudes cannot be compared between regions since the spectra were computed using the raw waveforms. Low-frequency earthquake (LFE) (red) and tremor (purple) spectra from Japan are highly similar, but tremor has smaller amplitude. Small (blue) and very small (cyan) earthquake spectra from both regions are highly similar to each other but lack the rapid decay of amplitude with increasing frequency that is characteristic of tremor, LFE, and noise (green) spectra.

tracked as the number of hours per day containing any tremor, regardless of the duration of tremor in a particular hour. During active periods of tremor in northern Cascadia and southwest Japan, bursts are observed in over half the hours of a day [McCausland *et al.*, 2005; Obara and Hirose, 2006]. In relatively inactive periods, tremor may only be observed in a few hours of a day. However, it should be noted that the actual percentage of an hour-long seismic record filled by tremor varies significantly; tremor can largely saturate an hour or occur only as several isolated minutes-long bursts. Recent work suggests that for northern Cascadia the total hours of tremor during an SSE is

proportional to the equivalent seismic moment of the event [Aguiar *et al.*, 2006]. Efforts to probe this relationship in southwest Japan are ongoing, but preliminary work indicates that a direct correlation between SSE size and tremor productivity is less apparent. Tremor productivity does vary between four regions of activity in southwest Japan, with the greatest activity occurring in western Shikoku followed by Tokai and Kii. Despite the possible connection with tremor productivity, reduced displacement amplitudes of tremor signals do not appear to be related to the size of the associated slip events [McCausland *et al.*, 2005; Rokosky *et al.*, 2006]. While it remains unclear what controls the duration and amplitude of tremor activity, detailed investigations of tremor signals compared with parameters like accompanying slow slip rate and inferred fluid presence may help elucidate the mechanism of tremor.

[20] Subduction zone tremor is generally characterized as low frequency because it has peak frequencies that are lower than local earthquake activity. Most tremor shows a rapid dropoff in frequency content above 6 Hz (Figure 5). Initial reports of tremor activity at subduction zones emphasized comparisons with volcanic tremor, especially in speculating about tremor sources. Although similarities between the two phenomena certainly warrant study, it is important to note that subduction tremor does not appear to be harmonic, a common feature in volcanic tremor. Figure 6 shows linear frequency-amplitude plots for western Shikoku subduction tremor and tremor associated with Costa Rica's Arenal volcano. Whereas subduction tremor shows high amplitudes at frequencies between 1 and 8 Hz, Arenal tremor has distinct peaks at 2, 3, and 4 Hz. To date, no work has shown convincing evidence that subduction tremor has a harmonic element, which decreases the likelihood that subduction tremor is the result of resonance phenomena, a frequent proposal for volcanic tremor. Hydrofracturing during fluid migration [Katsumata and Kamaya, 2003] and shear failure on the plate interface [Obara and Hirose, 2006; Shelly *et al.*, 2006] are alternative mechanisms that have been proposed for nonvolcanic tremor.

[21] In southwest Japan, impulsive arrivals (generally *S* waves) are occasionally embedded in tremor and sometimes cataloged by the Japan Meteorological Agency (JMA) as low-frequency earthquakes (LFE). In Cascadia, records of tremor do not exhibit such impulsive arrivals. The quality discrepancy between Japanese borehole stations and surface stations used in North America may obscure the ability to see small-amplitude arrivals in the Cascadia traces. Where studied, it appears that subduction tremor moves with *S* wave velocities (~ 4 km/s), which is consistent with the observed concentration of energy on the horizontal components [Obara, 2002; Rogers and Dragert, 2003]. Tremor has also been shown to propagate with slow slip in Cascadia and western Shikoku, Japan. However, propagation velocities vary between 5 and 15 km/d in these regions and are often sporadic.

[22] Tremor with similar characteristics has also been observed in the Parkfield region of the San Andreas Fault [Nadeau and Dolenc, 2005]. Although the mechanisms

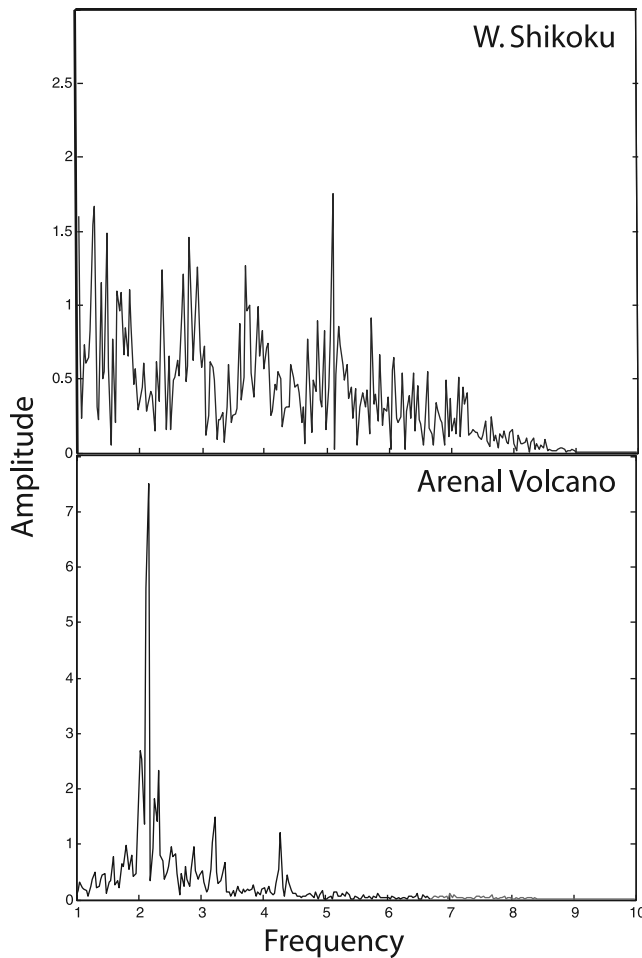


Figure 6. Linear-scaled plots of the frequency content between 1 and 10 Hz for tremor from western Shikoku, Japan, and Arenal Volcano, Costa Rica, whereas Arenal tremor shows distinct peaks at evenly spaced frequencies, indicating harmonic behavior, subduction tremor lacks such peaks.

behind subduction and continental fault tremor are not necessarily identical, similarity between the two phenomena argues for a relationship. What we know about the deep structure of the San Andreas Fault as well as the ongoing detailed study of the region may help elucidate the cause(s) of subduction tremor, so comparative study should be pursued.

3.3. Observations of Slow Slip and Tremor at Subduction Zones

3.3.1. Cascadia

[23] The Cascadia subduction zone, extending 1000 km from British Columbia to northern California, has a history of generating $M_w > 8.0$ earthquakes approximately every 300–500 years, with the last great earthquake occurring in 1700 [Satake *et al.*, 2003]. Geodetic measurements made over the last decade have shown that the plate interface along this entire segment is locked from near the surface to a depth of about 20 km [Wang *et al.*, 2003]. This region of geodetic locking has been identified as the seismogenic

zone. One of the earliest observations of a subduction zone SSE was made along the northern portion of the Cascadia margin from continuous GPS data [Dragert *et al.*, 2001]. These data revealed that in the fall of 1999 the contractional motions indicative of strain accumulation, at seven sites in southern Vancouver Island and western Washington, suddenly reversed their motion for a period of about 2 weeks at each station (Figures 3b and 3c). Dragert *et al.* [2001] found that the surface displacement data associated with this excursion could be well fit by ~ 2 cm of slow slip on a deep portion of the plate interface just below the seismogenic zone. This SSE had the equivalent moment of an $M_w = 6.7$ earthquake. Following this discovery, careful analysis of the continuous GPS time series from this network dating back to 1992 revealed the occurrence of eight similar SSEs with an average recurrence interval of 13–16 months [Miller *et al.*, 2002]. Each SSE lasted between 2 and 4 weeks at a particular station, migrated across the array, and was consistent with the slip model obtained for the 1999 event, i.e., a few centimeters of slip on the deep portion of the plate interface (25–45 km), yielding equivalent moment magnitudes of 6.5–6.8 [Dragert *et al.*, 2004]. Table 1 lists the relevant parameters associated with 10 documented SSE events in the northern Cascadia margin. McGuire and Segall [2003] inverted the surface displacements of the 1999 Cascadia SSE to obtain a model of the spatial and temporal variations in its fault slip. They found a slip sequence that initiated at a depth of about 30–35 km in the southern portion of the fault plane, attained its maximum displacement and slip rate of ~ 8 cm and 1 m/yr within its first 20 days, respectively, and slowed to less than 0.5 m/yr for the following 15–20 days before propagating updip and along strike to the northwest. The entire slip sequence lasted over 50 days and had an equivalent moment magnitude of 6.9 [McGuire and Segall, 2003]. Melbourne *et al.* [2005] inverted the surface displacements from the 2003 Cascadia SSE for the spatial distribution of slip on the fault plane in three successive time periods. Although the details of the slip pattern differed from those of the 1999 SSE, both events took approximately 2 months, revealed patchy slip distributions consistent with bilateral rupture propagation, and concentrated slip at the downdip edge of the seismogenic zone near the sharp bend in the subducting Juan de Fuca plate. The 2003 SSE was smaller, with maximum slip of 4 cm and cumulative moment equal to an $M_w = 6.6$ earthquake. The more detailed analyses of the 1999 and 2003 SSEs indicated that like large earthquakes, SSEs also possess slip complexity and concentrate their slip at isolated patches like asperities along the fault plane. Sufficient information to determine whether or not the same patches slip in consecutive SSEs does not yet exist.

[24] Although SSEs do not radiate seismic energy *per se*, Rogers and Dragert [2003] did detect significant increases in seismically recorded ground vibration (seismic tremor) that correlated with six Cascadia slow slip events (Figure 3d). Because of the correspondence and regular recurrence of tremor and slow slip events in northern Cascadia, Rogers and Dragert [2003] termed this coupled phenomena epi-

sodic tremor and slip (ETS). Although early work in northern Cascadia assumed that tremor sources were concentrated near the plate interface [Rogers and Dragert, 2003], more recent results indicate that the majority of tremor sources are distributed over a wide depth range between 20 and 40 km in the overriding continental crust [McCausland *et al.*, 2005; Kao *et al.*, 2005, 2006]. One exception was a 10 day tremor episode in February 2002 that located near the subduction interface [Royle *et al.*, 2006]. Tremor sources appear to be preferentially located where there are few local earthquakes, and they appear to be close to strong reflectors imaged in previous reflection profiles of the region [Kao *et al.*, 2006]. These reflectors are interpreted as regions of elevated fluid content, strengthening the connection between fluids and tremor nucleation. Tremor and slip appear to migrate together in time, although the locations and migration patterns vary between episodes. Recent ETS have shown bidirectional migration of slip and tremor sources during the multiweek episodes. Migration speeds varied between 5 and 15 km/d during the episodes. There appears to be no discernable migration in the vertical direction [Kao *et al.*, 2006].

[25] Continuous GPS and seismic data from northern California, Oregon, and southern Washington suggest that ETS occurs along the entire Cascadia margin. For northern California, Szeliga *et al.* [2004] detected 8 SSEs between 1997 and 2003 on the basis of GPS position changes from a single station; the most recent 5 SSEs were accompanied by seismic tremor recorded by seismic stations of the Northern California Seismic Network. The average value of the horizontal surface displacement during these events (4–6 mm) is similar to the northern Cascadia SSEs; however, their recurrence interval is 9–12 months, which is shorter than the 13–16 months obtained in northern Cascadia. Although GPS station coverage is too sparse to correlate SSEs between stations for all but the northern Cascadia margin, several single GPS stations along this margin show sudden reversals of motion that are consistent with SSEs. In most cases the correlation of sudden GPS motion reversals with seismic tremor episodes has been interpreted as strong evidence that they do represent slow slip on the subduction plate interface [Szeliga *et al.*, 2004; Brudzinski and Allen, 2006]. McCausland *et al.* [2005] identified many episodes of tremor between 2003 and 2006 recorded by groups of seismic stations located at different positions along the Cascadia margin. Some of these tremor episodes correlated with observed SSEs recorded by either a network of GPS stations in northern Cascadia or a single station in southern Cascadia [Brudzinski and Allen, 2006]. Although the data are very sparse between southern Washington and northern California, the SSEs in this region appear to have smaller surface displacements (<5 mm). Where enough consecutive observations of SSEs exist, Cascadia margin recurrence intervals appear to vary by region between 10 and 19 months. Regardless of the amplitude or recurrence interval of the slow slip, the general character of correlated tremor is the same; however, tremor amplitudes (measured as reduced displacements) do vary between episodes.

[26] In summary, the entire Cascadia margin appears to generate ETS with recurrence intervals that vary with location along the margin. Since all but the northern Cascadia SSEs are recorded at only a single GPS station, details of their locations, magnitudes, and migration patterns are unconstrained. Tables 1 and 2 summarize the main characteristics of the ETS observed along the Cascadia margin. Possible mechanisms generating these periodic events are discussed in section 5.

3.3.2. Southwest Japan

[27] Southwest Japan is a complex region of subduction where the Philippine Sea plate subducts beneath the Eurasian or Amurian plate along the Nankai and Sagami troughs and beneath the North American or Okhotsk plate along the Sagami Trough (Figure 7a). Great earthquakes and slow slip events occur along most of this subduction zone margin. There is a long history of great earthquakes along the Nankai Trough off Shikoku and the Kii Peninsula dating back over 1000 years with a recurrence interval of 90–150 years [Ando, 1975], while smaller events ($M_w < 7.5$) occur frequently to the southwest off of Kyushu. The most recent great earthquakes to rupture the Nankai Trough region occurred in 1944 ($M_w = 7.9$) and 1946 ($M_w = 8.0$). Several source studies of these events have been conducted using seismic, geodetic, and tsunami data, and the results indicate several regions of concentrated coseismic slip (asperities) on the shallow plate interface offshore of the Kii Peninsula and Shikoku [Sagiya and Thatcher, 1999; Kikuchi *et al.*, 2003; Tanioka and Satake, 2001]. The 1923 Kanto earthquake ($M_w = 7.9$) ruptured the plate interface between the Philippine and North American plates along the Sagami Trough in the Boso region. Wald and Somerville [1995] inverted seismic waveforms from this event to determine its asperity distribution, and Sato *et al.* [2005] recalculated the finite slip inversion using a refined plate geometry obtained from deep seismic reflection profiling. The Tokai region, between the 1944 and 1923 earthquake rupture zones, has not experienced a great earthquake since 1854 ($M_w = 8.4$) and is considered to be a mature seismic gap. Analysis of geodetic data over the past 100 years (leveling, triangulation, trilateration, sea level, and GPS surveys) indicates that between great earthquakes the plate interface in this region is accumulating strain. The strain accumulation pattern during the interseismic stage indicates a difference in plate locking across the Bungo Channel. The plate interface southwest of the Bungo Channel, which separates the islands of Shikoku and Kyushu, is weakly locked or slipping as compared to the plate interface to the northeast, which is accumulating strain at depths shallower than about 30 km [Ito *et al.*, 1999; Ito and Hashimoto, 2004]. In addition to strain accumulation and release in large to great earthquakes, slow slip events have been documented along much of the southwestern Japan subduction zone from network GPS observations, specifically in the Bungo Channel, Tokai, and Boso regions (Figures 7a and 7b). The existence of a very dense network of borehole tiltmeters throughout Japan since about 2000 (National Research Institute of Earth Science and Disaster Prevention

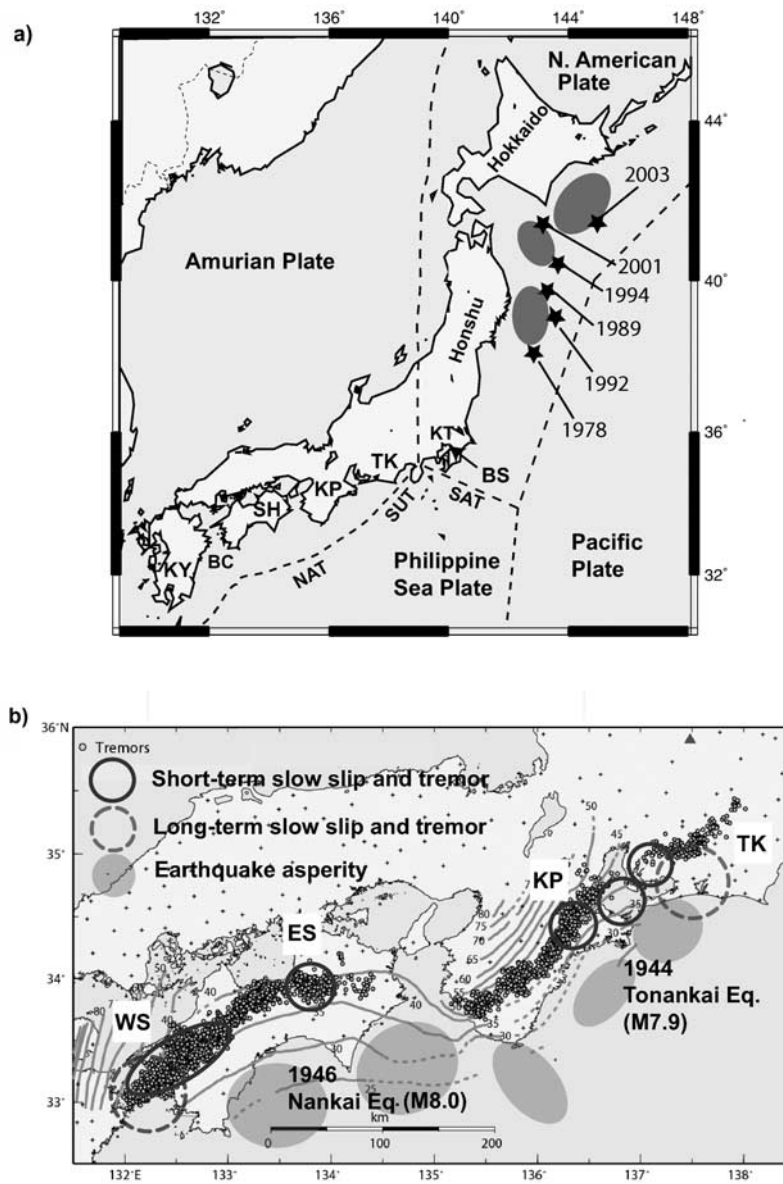


Figure 7. (a) Plate tectonic setting of Japan showing the location of six earthquakes (stars) in northeast Japan that were followed by significant afterslip and are listed in Table 1. Shaded ovals indicate regions that are locked during the interseismic stage and concentrate slip during large earthquakes (asperities). Afterslip locates in more freely slipping regions around these patches. KY, Kyushu; BC, Bungo Channel; SH, Shikoku; KP, Kii Peninsula; TK, Tokai; KT, Kanto; BS, Boso; NAT, Nankai Trough; SUT, Sagura Trough; and SAT, Sagami Trough. (b) Spatial distribution of short- and long-term slow slip, great earthquake asperities, and seismic tremor in southwest Japan. WS and ES are western and eastern Shikoku, respectively.

Hi-net array) has allowed very small SSEs, not recorded by surface GPS stations, to also be detected. Although these tilt changes are too small to be recognized as significant on their own, their strong correlation and migration with seismic tremor (Figure 8) indicate that they are related phenomena, and by their association with ETS at Cascadia they are believed to reflect slow slip on the plate interface [Obara *et al.*, 2004]. The patterns of strain accumulation and release in this area are indicated in Figure 7b, and details of the SSEs and associated seismic tremor are discussed further in this section.

[28] Seismic tremor is common along the subduction margin in southwest Japan, and it is the location where the phenomenon was first identified [Obara, 2002]. Tremor appears to peak during slow slip episodes observed in GPS and tiltmeter records (Figure 8). The most robust slip and tremor activity occurs in western Shikoku; however, peaks in tremor and concurrent minor slip episodes have been observed in eastern Shikoku, Kii Peninsula, and Tokai [Obara and Hirose, 2006; Hirose and Obara, 2006]. The character of tremor is relatively consistent between these

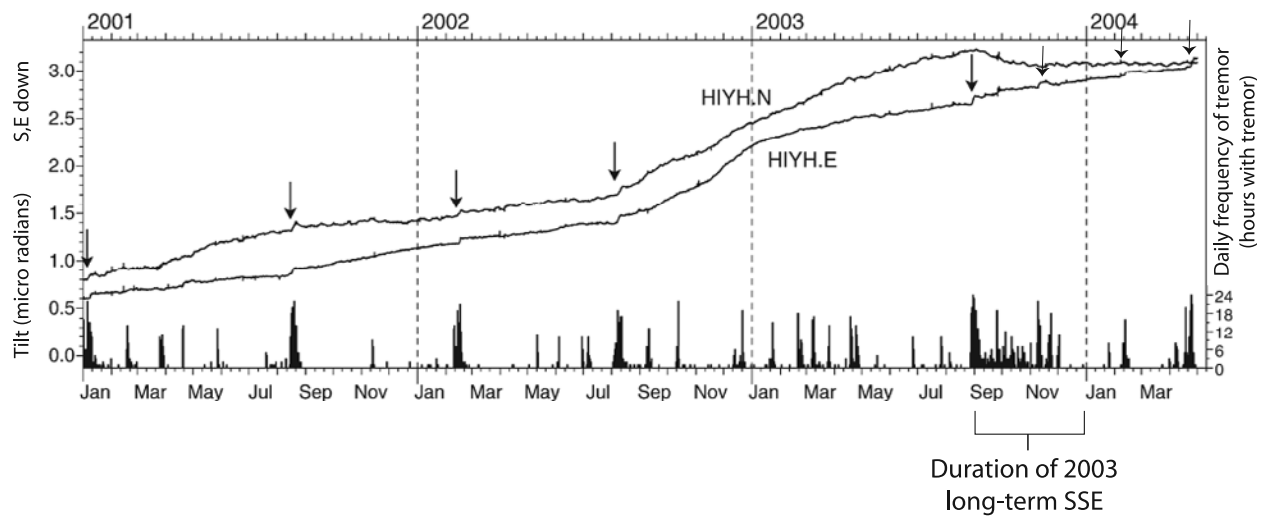


Figure 8. Histograms of hours with tremor per day for the western Shikoku region modified from *Obara and Hirose* [2006] with permission from Elsevier. The north and east tilt records from Hi-net station HIYH are superimposed, and arrows indicate short-term slow slip events identified by *Hirose and Obara* [2006] that correlate with peaks in tremor activity. The long-term Bungo Channel slow slip event began in August 2003 and corresponds to the highest concentration of tremor in the studied period.

regions, although productivity (hours/days) appears to differ significantly.

[29] *Obara* [2002] used a cross-correlation technique to locate tremor in southwest Japan by tracking the differential arrival times of tremor envelopes. In contrast, the JMA calculates the location of what they refer to as low-frequency earthquakes within tremor via traditional methods using the enlarging part of the signal as a discrete arrival [*Katsumata and Kamaya*, 2003]. Both these methodologies locate tremor sources between 25 and 40 km in a diffuse 30–50 km wide, belt-like distribution parallel to the subducting Philippine plate (Figure 7b). These locations suggest that tremor is sourced in the crust of the overriding plate, near the junction between the Moho and the subducting lithosphere. The location of tremor in the continental crust near the inferred locations of slab dehydration suggests tremor source mechanisms that involve fluids, as has been suggested for Cascadia. In addition, some work suggests that tremor sources cluster near regions of high V_p/V_s ratios, strengthening the connection to fluids [*Kurashimo and Naoshi*, 2004; *Matsubara et al.*, 2005; *Shelly et al.*, 2006].

[30] *Shelly et al.* [2006] used waveform cross correlation to identify impulsive P and S arrivals in LFEs embedded in tremor and to calculate differential traveltimes between stations to obtain LFE hypocenters. This technique yielded a concentrated pattern of LFE sources in a plane parallel to the inferred top of the subducting Philippine plate and led the authors to argue that LFEs are generated by shear dislocation on the plate interface. By using well-located LFEs as template events, *Shelly et al.* [2007] systematically searched tremor signals to detect matching waveforms at multiple stations. This technique revealed a nearly continuous sequence of detected LFEs during times of active tremor, establishing that nonvolcanic tremor beneath Shikoku, Japan, can be explained by a swarm of LFEs, with

each event most likely caused by shear failure on the plate interface.

[31] Finally, in addition to tremor occurring during slow slip episodes it also appears to be triggered by passing surface waves from distant earthquakes. However, triggering is not a persistent feature and appears to be strongly dependent on current stress conditions [*Miyazawa and Mori*, 2005, 2006]. As will be discussed in section 5.2, the correlation of tremor bursts with peaks in the dilatational stresses imposed by passing Rayleigh waves suggests that minute changes in the local stress field can result in the triggering of tremor if the system is primed (for example, by an abundance of fluids).

3.3.2.1. Bungo Channel and Western Shikoku

[32] The first GPS deformation signal to be interpreted as a slow slip event was recorded by the Japanese nationwide GPS Earth Observing Network (GEONET) between 1996 and 1998 in the Bungo Channel region of southwestern Japan [*Hirose et al.*, 1999]. A sudden reversal of surface displacements at several stations in the vicinity of the Bungo Channel, initiating in early 1997 and lasting ~ 300 days, suggested slow slip on the plate interface (Figure 7b). *Hirose et al.* [1999] modeled the surface displacement pattern and found that it was best fit by variable slip between 5 and 18 cm over a 60×60 km² fault area with most slip occurring between 30 and 40 km depth, downdip of the seismogenic zone [*Hyndman et al.*, 1995]. This model yielded an equivalent earthquake moment magnitude of 6.6 with an average slip velocity on the order of 0.03 m/yr. *Miyazaki et al.* [2003] applied the full network inversion filter to the surface displacement field to determine a time varying slip model for this event. They also found that most of the slow slip occurred on the plate interface in the depth range of 30–40 km; however, they documented southwest and updip migration of slip and obtained a much larger total moment, equivalent to an $M_w = 7.2$ earthquake. Similar

slow slip recurred in August 2003, as reported by *Ozawa et al.* [2004]. They applied Kalman filtering to invert the GPS observations for the spatial and temporal distribution of slow slip on the fault plane and found a very similar slip distribution to that of the 1997 SSE and an equivalent earthquake magnitude of $M_w = 7.0$. During both events, slip concentrated at the transition in plate coupling from locked in the northeast to more freely slipping in the southwest. The more freely slipping plate interface, about 100 km southwest of the Bungo Channel SSEs, experienced significant afterslip following two 1996 $M_w = 6.7$ Hyuganada earthquakes that occurred within 3 months of the onset of the 1997 SSE. *Miyazaki et al.* [2003] included GPS data spanning these earthquakes, in both time and space, in their slip inversion and found that moment released as afterslip ($M_w = 6.9$) within a year of the first earthquake exceeded the coseismic moment release of each event ($M_w = 6.7$). They also showed that the area of afterslip did not extend into the source region of the 1997 SSE, indicating that although the 1996 Hyuganada earthquakes and the 1997 SSE may have been related through static stress transfer, they represent two distinct occurrences. In addition, because no similar activity occurred during the 2003 SSE, it seems unlikely that afterslip in Hyuganada was a driving factor in slow slip initiation in 1997.

[33] Eight episodes of tilt change that correlate with increased seismic tremor activity have been observed in western Shikoku between 2001 and 2005 (Figure 8) and have been interpreted as short-term SSEs, lasting on the order of days to a week [*Obara et al.*, 2004; *Hirose and Obara*, 2005; *Obara and Hirose*, 2006]. The longer-duration (~ 3 months) 2003 Bungo Channel SSE described above temporally overlaps two of these eight events. Dislocation modeling of the tilt data at several stations has allowed source parameters of five of the short-term SSEs to be determined [*Obara et al.*, 2004; *Hirose and Obara*, 2005; *Obara and Hirose*, 2006]. In general, the short-term SSEs locate at the downdip edge of the plate interface at depths between 20 and 45 km, a bit deeper than the long-term 1997 and 2003 SSEs (Figure 7b). Their source areas appear to define several patches on the deep plate interface with each SSE activating a slightly different combination of these patches [*Hirose and Obara*, 2005]. The average slip in each event is between 1 and 3 cm, yielding equivalent moment magnitudes between 5.8 and 6.2 and average slip rates between 0.5 and 1 m/yr, which is comparable to the long-term SSEs. While the long-term SSEs seem to repeat every 6 years, the recurrence interval for short-term SSEs is 2–6 months, with the four earliest SSEs that occurred prior to the initiation of the 2003 long-term SSE having the longer repeat intervals of 6 months (Figure 8). The occurrence of the 2003 long-term slow slip event appears to have shortened the interval time between short-term slip episodes and was itself related to a general elevation in tremor activity [*Hirose and Obara*, 2006]. Peaks in tremor apparently precede tilt changes by several days, but imprecision in the tiltmeter record limits this observation. Tremor migrates across the region during the week-long episodes, with an

apparent seasonal variation in direction (NE to SW in winter, SW to NE in summer). This alternating migration correlates with seasonal differences in crustal deformation; when tremor is in the NE, tilt is south down, and when tremor is in the SW, tilt is southeast down [*Obara and Hirose*, 2006]. Although tremor is distributed in depth, tremor sources are generally concentrated near the updip limit of slow slip.

3.3.2.2. Eastern Shikoku

[34] The occurrence of frequent small SSEs has been suggested by *Obara and Hirose* [2006] on the basis of periodic tremor activity that lasts ~ 3 –5 days, repeats every 2–3 months, and is sometimes accompanied by tilt changes at nearby stations. If slow slip on the plate interface is responsible for the correlated tilt and seismic signals, the small changes in tilt observed require these SSEs to be smaller than the short-term SSEs recorded in western Shikoku. Too few tilt observations exist to locate the SSEs. However, the associated seismic tremor locates downdip of a portion of the 1946 Nankai ($M_w = 8.0$) rupture zone (Figure 7b).

3.3.2.3. Kii Peninsula

[35] Similar to eastern Shikoku, episodes of correlated tilt changes at a single or a few stations and seismic tremor occur approximately every 6 months beneath the northern Kii Peninsula and have been interpreted as episodic SSEs [*Obara and Hirose*, 2006]. Although not as well studied as western Shikoku, Kii Peninsula ETS appears to migrate at ~ 10 km/d. On the basis of locations of the tremor episodes the slow slip appears to locate along the plate interface downdip of the 1944 Tonankai ($M_w = 7.9$) rupture area (Figure 7b).

3.3.2.4. Tokai

[36] Continuous GPS data from GEONET stations in the Tokai region (Figures 7a and 7b) between 1996 and mid-2000 contain a strain accumulation signal consistent with locking on the Philippine and Amurian plate interface in the depth range of 10–25 km [*Ohta et al.*, 2004; *Miyazaki et al.*, 2006]. This strongly coupled region corresponds very well with the expected rupture zone of the future Tokai earthquake. These GPS data show a change in direction and deformation rate beginning in mid-2000 that persists through the first half of 2006 and is consistent with slow slip on the deeper portion of this plate interface in the depth range of 25–40 km (Figure 7b), at a rate that varies between 0.03 and 0.11 m/yr [*Ozawa et al.*, 2002; *Ohta et al.*, 2004; *Miyazaki et al.*, 2006]. *Miyazaki et al.* [2006] inverted the GPS data in the time range between January 2000 and November 2002 for the spatiotemporal distribution of slow slip on the fault plane. Their results indicated two slow subevents with slip that accelerated and decelerated several times but concentrated downdip of the portion of the fault plane previously determined to be strongly coupled. The maximum slip attained in this time period was ~ 14 cm, which is equivalent to an earthquake of $M_w = 6.8$; however, the SSE continued for several more years, eventually attaining an M_w larger than 7.0. Analysis of tilt observations at a single station in the region between 1981 and the

present revealed anomalous tilt associated with the recent Tokai SSE as well as a nearly identical anomaly between 1988 and 1990 [Yamamoto *et al.*, 2005]. Yamamoto *et al.* [2005] interpreted the 1988–1990 signal as an SSE and speculated that SSEs in the Tokai region occur repeatedly. However, they noted that the size and duration of the recent SSE far exceeds its predecessor and that variations in SSEs in this region must exist.

[37] Two short-term SSEs with accompanying peaks in seismic tremor were detected in 2004 and 2005 in two distinct areas in the Tokai region, the Shima Peninsula of the northern Kii Peninsula, and Aichi [Hirose and Obara, 2006]. These events had durations of 2–3 days, equivalent moment magnitudes of $M_w \sim 6.0$, and repeat times of about 6 months. Events in the Aichi region followed those in Shima by 1–2 weeks [Hirose and Obara, 2006], possibly representing slow slip migration between these regions. Earlier peaks in tremor were also detected in this area [Obara, 2002; Ohta *et al.*, 2004; Obara and Hirose, 2006].

3.3.2.5. Boso

[38] Continuous GPS data for the period between June 1996 and May 2000 from the Kanto district of Japan (Figure 7a) indicate northwestward motion and subsidence, consistent with strain accumulation on the plate interface. Inversion of the surface displacement rates for coupling on the plate interface reveals locking in the western Sagami Trough at depths shallower than 20 km [Sagiya, 2004]. The locked region encompasses the asperities of the 1923 Kanto earthquake, determined by Wald and Somerville [1995], but extends farther to the east. GPS data in the time period between May and June 1996 reveal anomalous horizontal motions on the eastern Boso Peninsula that have been interpreted as a slow slip event [Sagiya, 2004]. Inversion of these data for the distribution of the slow slip indicates that ~ 5 cm of slip occurred on a 50×50 km² patch of the fault plane within a period of ~ 1 week, yielding an equivalent moment magnitude of 6.4 and a slip rate of ~ 3 m/yr. The source region of the slow slip event occurred on the plate interface at a depth between 10 and 20 km, identical to that of the interseismic locking and the 1923 Kanto earthquake asperity, however, in a different location along strike farther to the east. This is unusual in that all other interseismic SSEs discussed thus far locate down dip of the regions of interseismic locking and coseismic rupture. The source area of this SSE locates at the boundary between a locked and a more freely slipping region of the plate interface that corresponds to a large contortion in the downgoing Philippine Sea plate, perhaps because of its interaction with the westward subducting Pacific plate. A second slow slip event was documented in this region over a 50-day period beginning in October 2002 [Ozawa *et al.*, 2003]. Ozawa *et al.* [2003] inverted the GPS data to obtain the time evolution of the 2002 Boso event and to compare it with characteristics of the SSE 6 years prior. They found that the magnitude of the 2002 event ($M_w = 6.6$) exceeded the 1996 event, and although their slip areas overlapped, the centroid of slip during the 2002 event located farther to the

south. Slow slip in this region does not appear to be accompanied by significant tremor activity.

3.3.3. Northeast Japan

[39] Strain release along the Pacific-North American (or Okhotsk) plate interface in northeast Japan occurs as great earthquakes, many of which experienced significant amounts of afterslip, and continuous aseismic slip with no documented observations of interseismic slow slip events. Suwa *et al.* [2006] inverted both the horizontal and vertical components of GEONET data to obtain the pattern of interseismic strain accumulation on the plate interface in northeastern Japan. They found a few locked patches that extended to about 60 km in depth beneath north central Honshu and somewhat deeper beneath Hokkaido (Figure 7a). A comparison of this pattern of interplate strain accumulation with the asperity distribution for all earthquakes with $M_w > 7.5$ in this region determined by Yamanaka and Kikuchi [2003, 2004] reveals a very close correspondence. This indicates that the regions of maximum coseismic slip during large earthquakes heal very quickly and become the loci of strain accumulation in the interseismic period. The significant afterslip that followed the 1994 Sanriku-Oki ($M_w = 7.7$) and 2003 Tokachi-Oki ($M_w = 8.0$) earthquakes was discussed in section 2.1.1 and was found to primarily occur in regions that slip at or near the plate rate during interseismic periods. Afterslip following smaller earthquakes in this region has also been detected by strainmeters for the 1989 ($M_w = 7.4$) and 1992 ($M_w = 6.9$) Sanriku-Oki earthquakes [Kawasaki *et al.*, 1995, 2001], by tide gauge and leveling for the 1978 Miyagi-Oki ($M_w = 7.4$) earthquake [Ueda *et al.*, 2001], and by GPS for the moderate-sized 2001 ($M_w = 6.4$) Tokachi-Oki earthquake [Sato *et al.*, 2004]. It appears that afterslip on the plate interface occurring in regions that slip near the plate rate in the interseismic period is a common occurrence following moderate to great earthquakes. The portions of the fault plane that host earthquake afterslip also generate a large number of small repeating earthquakes [Igarashi *et al.*, 2003]. Repeating earthquakes have nearly identical waveforms recorded at the same stations, indicating that they rupture similar fault locations. Repeating earthquakes were first observed along the San Andreas Fault system in California and were interpreted as the repeat rupture of small isolated asperities embedded within freely slipping regions [Nadeau and Johnson, 1998]. Uchida *et al.* [2003] contoured the distribution of repeating earthquakes on the plate boundary in northeastern Japan and found several concentrations of repeating earthquakes that they interpreted as freely slipping portions of the plate boundary. A comparison of the repeating earthquake clusters with the geodetically determined distribution of plate coupling confirms that they do occur where the plate interface is freely slipping. In summary, the plate interface in northeastern Japan appears to be composed of (1) regions that are accumulating strain at rates close to plate convergence that will become the loci of future large earthquakes (Figure 7a), (2) regions that are continuously slipping at or near plate rates, and (3) regions that slip at intermediate rates somewhere between that of earthquakes and plate rates but only

when driven by coseismic slip in adjacent regions (these are regions of afterslip). Although several different modes of strain release are observed, there is no evidence of episodic SSEs during the interseismic period in northeast Japan. LFEs occur in northeast Japan but are concentrated near volcanoes and do not appear to be correlated with slow slip. It remains unclear if any correlation exists between this activity and postseismic slip of earthquakes near volcanic regions.

3.3.4. Mexico

[40] Subduction of the Cocos plate beneath the North American plate along the Middle American Trench in Mexico generates large to great earthquakes every 30–100 years. The last great earthquake that occurred along the Guerrero segment in southern Mexico was in 1911, making it a likely location for rupture during a future large earthquake. Data from a single continuous GPS station in the Guerrero region recorded transient surface displacements in early 1998 that were interpreted as slow slip on the plate interface [Lowry *et al.*, 2001]. The continuous GPS data from this station, campaign data from several other stations in the area, and leveling data were consistent with moment release equivalent to an $M_w \geq 6.5$ earthquake that propagated along strike over several months. In 2001, seven permanent GPS stations in the Guerrero region recorded a reversal of surface motion consistent with a SSE beginning in October 2001, lasting approximately 7 months with an $M_w = 6.8$ –7.5. The large range in size estimate for this event resulted from the use of different modeling techniques. A finite fault modeling approach that solves for slip on a discretized plane yielded $M_w = 6.8$, while a single patch modeling method produced $M_w = 7.5$ with exactly the same data [Lowry *et al.*, 2005]. Lowry *et al.* [2005] recognized this problem and suggested caution when comparing the size and locations of SSEs determined by using different techniques. Campaign and continuous GPS data collected in the Guerrero region between 1992 and early 2001 were inverted to obtain both the interseismic deformation pattern and the location of transient slip events during this period. The pattern of interseismic strain accumulation indicated a locked plate interface at depths shallower than 25 km, and modeling of reversals of this motion indicated SSEs in 1995–1996 ($M_w = 6.8$ –7.1) as well as in 1998 ($M_w = 6.8$ –7.1) that both occurred at depths below 25 km [Larson *et al.*, 2004]. Lowry *et al.* [2005] detected additional SSEs along this plate boundary in 1999, 2000, 2001, 2003, and 2004, yielding a total of eight SSEs within 9 years and producing an average recurrence interval of approximately 1.1 years. Only the 2001–2002 SSE had a well-determined location with up to 30 cm of slip on the plate interface concentrated below 25 km, which is below the region of strong interseismic coupling. Seismic coverage is currently not sufficient to assess whether tremor activity occurs in Guerrero; however, deployments are scheduled that will help address this deficiency.

3.3.5. New Zealand

[41] The Hikurangi Trough, off the east coast of the North Island of New Zealand, marks the boundary between

the obliquely subducting Pacific plate and the Australian plate. The interseismic strain accumulation pattern, inferred from campaign GPS data, indicates a shallowing in the depth and a reduction in the degree of locking of the plate interface from the southern tip of the North Island northward [Wallace *et al.*, 2004]. Since 2002, several slow slip events of variable size and duration have been inferred to occur along the Hikurangi margin on the basis of continuous GPS records [Beavan *et al.*, 2007]. A reversal of surface displacements over a 10 day period in October 2002 at two GPS stations near Gisborne, on the northeast coast of the North Island, was the first reported SSE in this region [Douglas *et al.*, 2005]. The surface displacements were modeled by 18 cm of slip on the plate interface at the downdip edge of the seismogenic zone. A similar reversal of motion observed at the end of 2004 and analysis of campaign GPS data between 1995 and 2004 suggested that SSEs in this region may have a recurrence interval of 2–3 years [Douglas *et al.*, 2005]. The largest SSE was recorded on seven continuous GPS stations in the Manawatu region of the southern North Island beginning in early 2004 and lasting ~ 18 months [Wallace and Beavan, 2006]. Inversion of the horizontal and vertical displacement field yielded a model of up to 35 cm of slip at the downdip edge of the seismogenic zone, at a position coincident with the sudden change in interface properties from locked to more freely slipping [Wallace and Beavan, 2006]. Smaller changes in surface displacements, detected on a few GPS stations in the intervening region between Gisborne and Manawatu, occur frequently (at least one each year), last about a month, and have also been interpreted as slow slip events on the plate interface at the downdip end of the seismogenic zone [Beavan *et al.*, 2007]. Several of these SSEs occurred close enough in time to the larger Gisborne and Manawatu SSEs to suggest an along-strike migration of slip during these larger events. No coincident tremor has been reported for this region, but seismic data have only been systematically examined following the 2004 Gisborne SSE [Delahaye *et al.*, 2006]. Although the apparent diversity in characteristics of Hikurangi subduction zone SSEs over such short time and distance scales holds much promise for contributing to our understanding of aseismic plate motions, the observations made thus far are sparse and the details of slow slip events in this region must await further confirmation.

3.3.6. Costa Rica

[42] The Nicoya Peninsula in northwestern Costa Rica is located along the Middle America Trench where the Cocos plate subducts under the Caribbean plate at about 8 cm/yr [DeMets, 2001]. This subduction segment has ruptured in the past with large earthquakes in 1853, 1900, and 1950. It is presently recognized as a mature seismic gap with the potential to generate an $M_w > 7.5$ earthquake in the near future [Pratti *et al.*, 2001]. The Nicoya peninsula lies directly over the seismogenic zone, allowing precise recording of crustal deformation associated with locking of the shallow plate boundary. A dense network of campaign GPS measurements between 1991 and 2003 has allowed the

lower extent of the locked seismogenic zone as well as the pattern of strain accumulation on the plate boundary to be estimated [Lundgren *et al.*, 1999; Iinuma *et al.*, 2004; Norabuena *et al.*, 2004]. These data have revealed that seismic coupling is spatially heterogeneous with a locked region offshore the Nicoya Peninsula at a depth of ~ 12 km with essentially no background seismicity during the interseismic period, transitioning downdip to a relatively freely slipping region with abundant microseismicity. Three GPS stations on the Nicoya Peninsula recorded a transient deformation event lasting approximately 1 month in September–October 2003. The transient displacements are nearly opposite in direction to plate convergence and strain accumulation on the plate interface and appear to have initiated at the updip transition from a locked to more freely slipping interface and propagated landward (downdip). The transient displacements have been interpreted as a SSE located primarily within the seismogenic zone [Protti *et al.*, 2004]. The data are too limited to resolve details of the slip event, but a simple dislocation model suggests that the observations can be explained by an average of 1.5 ± 0.5 cm of slip on the plate interface. It is possible that this region of the plate boundary, part of which appears to be slowly creeping in campaign GPS data (temporally averaged over nearly a decade), may, in fact, alternate between a locked state and slow slip events.

[43] Three SSEs in early 2000, lasting approximately 3 weeks each, may have occurred in the Nicoya region; this conclusion is based on observations of correlated transient fluid flow and seismic tremor [Brown *et al.*, 2005]. Brown *et al.* [2005] proposed a model where the poroelastic stress/strain field from creep dislocations along the shallow thrust fault force flow through fracture networks in the forearc and oceanic basement, generating seismic tremor recorded by ocean bottom seismometers collocated with the fluid flowmeters and inducing diffuse flow through shallow sediments to produce fluid flow transients. Although Brown *et al.* [2005] could not precisely locate the postulated SSEs, the magnitude and timing of the fluid flow excursions argue for updip slip propagation extending to depths of only 1–2 km below the ocean floor; no constraints could be placed on the downdip extension of slip. The GPS time series are too short to assess the repeat interval, if any, for Costa Rica events, but evidence for three SSEs in 2000 and 2003 suggest that this mode of strain release may be common along the Nicoya segment of the Costa Rica subduction zone.

[44] During the September 2003 SSE, three broadband, three-component seismic stations were operating on the Nicoya Peninsula. One seismic station was collocated with a continuous GPS station; however, the other two seismic stations were quite far from the best determined location of the slow slip event. We processed the continuous seismic data from all three Nicoya stations following the procedure used to identify episodic tremor in the Cascadia subduction zone. We found no tremor signals that correlated between stations. Perhaps this is not surprising given the small amplitude of expected signals and the large interstation spacing. A denser network of both continuous GPS and

seismic stations is required to rigorously assess the spatial pattern of slow slip and to enable an evaluation of the relationship between slow slip and seismic tremor. Such a network is currently operating on the Nicoya peninsula.

3.3.7. Alaska

[45] The eastern end of the Alaska–Aleutian subduction zone is the site of the great $M_w = 9.2$ 1964 Prince William Sound earthquake. This event ruptured a large region of the shallow plate interface above 30 km depth and had a long and complicated postseismic deformation history [Cohen and Freymueller, 2004]. Ohta *et al.* [2006] inverted GPS data for the period between 1997 and 2002 and found two distinct deformation patterns. Data before 1998 and after 2001 showed surface displacements consistent with strain accumulation over the entire shallow plate interface while data between 1998 and 2001 indicated continued strain accumulation on the shallow plate interface and a SSE on the deeper interface in an isolated region north of Anchorage. The region with the largest slip deficit or maximum locking lies beneath the southeast Kenai Peninsula and corresponds to the asperity that broke in the 1964 earthquake. During the period between 1998 and 2001 the surface velocities north of Anchorage changed compared to the other time periods and are consistent with the occurrence of a SSE. The best fitting fault parameters for this SSE were found to be maximum and average slip rates of 55 and 40 mm/yr, respectively, producing total slip of 120–165 mm over a fault area of $\sim 150 \times 150$ km² for the 3 year event duration. The cumulative seismic moment was 1.1×10^{20} Nm, which corresponds to $M_w = 7.2$ [Ohta *et al.*, 2006]. The maximum slip area of the SSE locates at depths between 25 and 45 km, just below the seismogenic zone.

[46] Peterson *et al.* [2005] report seismic tremor at stations spanning over 100 km along the Alaska–Aleutians Trench. Although work is ongoing to more fully characterize it, tremor is similar in nature to activity in Cascadia and appears to source above the 40–50 km contour of the subducting Pacific plate in the region of the SSE. Whether tremor is uniquely associated with the SSE or occurs before and after is currently being investigated.

3.3.8. Slow Slip in the Accretionary or Forearc Margin Wedge of Subduction Zones

[47] As discussed in section 3.3.6, Brown *et al.* [2005] postulated that SSEs at shallow depth below the Costa Rican forearc margin wedge were responsible for three episodes of correlated fluid flow and seismic tremor recorded on the seafloor in 2000. The existence of shallow slow slip at subduction zones was also suggested by Davis *et al.* [2006] on the basis of a transient in fluid pressure recorded in two boreholes offshore eastern Shikoku, Japan, in 2003. A swarm of very low frequency (VLF), reverse-faulting earthquakes within the adjacent accretionary prism [Ito and Obara, 2006a] occurred concurrently with this pressure transient. These VLF events have stress drops that are less than 1% of ordinary earthquakes, suggesting that fluids may be involved in fault zone weakening [Ito and Obara, 2006b]. Davis *et al.* [2006] postulated that both the VLF earthquakes and the fluid pressure transient were triggered by a slow slip event that

initiated at the updip frictional transition and propagated seaward toward the trench for approximately 10 days. Observations of similar VLF events at the downdip transition zone of the Nankai plate interface that accompany and migrate with deep seismic tremor and SSEs [Ito *et al.*, 2006] lend support to the connection between VLF and slow slip events. Stress changes imposed on sensitive aquifers by either seismic events or slow slip events can lead to transient pore pressure gradients. These seafloor observations of SSEs suggest that shallow slow slip may be quite common but largely undetected because of the absence of monitoring instrumentation. Efforts to establish long-term hydrologic and geophysical borehole observatories on the seafloor in other locations are in the planning stages; these efforts coupled with advances in seafloor geodetic techniques promise to fill this gap in our knowledge of offshore deformation.

3.4. Observations of Slow Slip and Tremor Elsewhere

3.4.1. San Andreas Fault

[48] Aseismic strain transients have been identified along the San Juan Bautista and Parkfield segments of the San Andreas Fault [e.g., Linde *et al.*, 1996; Langbein *et al.*, 1999]. The Parkfield event was associated with abrupt changes in electronic distance meter line length measurements, tensor strain, and a 30% increase in slip rate on the fault inferred from the recurrence interval of repeating earthquakes between early 1993 and lasting until 1996 [e.g., Linde *et al.*, 1996; Langbein *et al.*, 1999; Gao *et al.*, 2000; Nadeau and McEvilly, 1999; Murray and Segall, 2005]. Several slow slip events have been reported along the central San Andreas Fault near San Juan Bautista in 1992 [Linde *et al.*, 1996], 1996 [Johnston *et al.*, 1996; Johnston, 1997], 1998 [Gwyther *et al.*, 2000], 2003, and 2004 [Gladwin, 2004; Pollitz and Johnston, 2006]; however, only the first of these is well documented. This event lasted for only 5 days, but its slip sequence revealed complexities as great as those observed during normal earthquakes. The source processes consisted of several slip episodes scattered in the upper 8 km of ~ 50 km² fault plane with slip amplitudes and durations ranging from 0.3 to 2.5 cm and 0.6 to 43 hours, respectively [Linde *et al.*, 1996]. The total moment of this sequence was equivalent to an $M_w = 5$ earthquake.

[49] Seismic tremor was observed in the San Andreas Fault near Cholame, California, some 40 km south of Parkfield during the 3 year period preceding the December 2003 $M_w = 6.5$ San Simeon earthquake. Using the envelope method of Obara [2002], the tremors located at depths between 20 and 40 km, well below the seismogenic zone (~ 15 km). Peaks in tremor activity correlated with increased rates of microseismic activity [Nadeau and Dolenc, 2005]. The frequency content of the tremor is similar to subduction zone tremor summarized in sections 3.2 and 3.3, but tremor bursts along the San Andreas Fault are less frequent than during times of peak activity in southwest Japan and Cascadia.

3.4.2. Hawaii

[50] With a continuous GPS network on Kilauea volcano, Hawaii first recorded transient displacements in November

2000 that were interpreted as a SSE [Cervelli *et al.*, 2002]. Inversion of the GPS data indicated that slip occurred on a shallow dipping thrust fault at a depth of ~ 5 km beneath the southeast flank of the volcano. Slip attained a maximum rate of 6 cm/d and lasted for about 36 hours, producing 87 mm of total slip with an equivalent moment magnitude of 5.7 [Cervelli *et al.*, 2002]. A peak in rainfall 9 days before this SSE suggests a causal relationship. Cervelli *et al.* [2002] postulated that an elevated water table, resulting from nearly 1 m of rainfall in a short period of time, increased the pore pressure and decreased the effective normal stress on crustal faults triggering slip. Reexamination of 8 years of GPS data from Kilauea revealed three additional slow slip events that were not associated with periods of increased rainfall [Brooks *et al.*, 2006]. While source parameters for the new SSEs could not be uniquely determined, their GPS data are consistent with motion on a shallow reverse fault, similar to the model proposed by Cervelli *et al.* [2002] with comparable seismic moments. These four SSEs appear to be periodic with a recurrence interval of 774 ± 7 days. Brooks *et al.* [2006] suggested that a cycle of aquifer recharge, pressurization, slow slip, aquifer rupture, and repressurization might be responsible for the periodicity of the slow slip events. Work is ongoing to identify tremor concurrent with this slow slip event, but limited seismic data make identification difficult.

3.5. Observational Summary

[51] Slow slip events in subduction zones, either occurring in the interseismic stage or as afterslip, overwhelmingly locate in the frictional stability transition zone (Figure 1a). Notable exceptions include the 1996 and 2002 Boso and 2003 Costa Rica interseismic SSEs and afterslip following several large earthquakes in northeastern Japan and the 2005 Nias and 2004 Sumatra, Indonesia, earthquakes. In these cases, slow slip occurred within the seismogenic zone but in complementary locations to strongly locked patches or coseismic asperities. This observation indicates that different frictional properties control the occurrence of fast versus slow slip. Rate- and state-dependent frictional modeling supports this, finding that SSEs require either spatially or temporally variable friction. Shibasaki and Iio [2003] were able to simulate SSEs by introducing temporal variations in their rate- and state-dependent frictional modeling such that steady state friction behaves as velocity weakening at low-slip velocity and velocity strengthening at high-slip velocity. Their simulated SSEs had slip velocities of tens of meters per year, propagated horizontally at rates of ~ 10 km/yr, and persisted for tens of years. Yoshida and Kato [2003] and Liu and Rice [2005] successfully simulated SSEs with spatially variable friction using block-spring models and three-dimensional numerical simulations, respectively. In the block-spring models, slow slip events occurred only in regions where friction was near the stability limit [Yoshida and Kato, 2003]. In the numerical modeling, SSEs appeared spontaneously at the downdip edge of the seismogenic zone, which Liu

and Rice [2005] attributed to the transition from unstable to stable frictional properties. These simulated strain transients had slip velocities that measured meters to tens of meters per year (1–2 orders of magnitude faster than plate velocities). Resulting slip was confined to the downdip frictional stability transition and migrated along strike at tens of kilometers per year over tens of years. Only the last characteristic is unlike most observations of SSEs in subduction zones in that it is longer than the observations. Transitions in frictional properties from velocity weakening to velocity strengthening seem to be required to generate SSEs. While we expect this transition at the downdip edge of seismogenic zones, where most SSEs occur, it appears likely that such transitions also exist within seismogenic zones (as illustrated in Figure 1b) and are the loci of slow slip nucleation. Along-strike variations in frictional properties were postulated as important in controlling patterns of afterslip in northern Chile [Pritchard and Simons, 2006].

[52] The few convergent margins that exhibit slow slip within their seismogenic zones (northeast Japan, Boso, and Costa Rica) share some other common features that may be important to understanding the generation of slow slip. In particular, the seismogenic zones of these plate boundaries, defined by the 350°C isotherm (believed to coincide with the frictional transition from velocity weakening to strengthening behavior) and/or the downdip limit of underthrusting earthquakes or geodetic locking, extend to depths below where the continental Moho intersects the downgoing plate (relatively cool plate interface temperatures). The three subduction zones that have well-located SSEs within the frictional transition zone (Cascadia, southwest Japan, and Guerrero, Mexico) have relatively hot plate interfaces where temperatures reach 350°C at shallow depths, above where the continental Moho intersects the subducting plates. Although it is unclear which attributes of these hot subduction zones are most important for deep slow slip generation, reaching the frictional transition at relatively low pressure or where oceanic crust of the downgoing plate is in contact with crust of the overlying plate appears to be required for deep slow slip. Cascadia and southwest Japan are the only two subduction zones where a convincing relationship between slow slip and seismic tremor has been established. It has been postulated that seismic tremor results from fluid movements in the crust generated from dehydration reactions in the oceanic slab [Katsumata and Kamaya, 2003; Seno and Yamasaki, 2003]. The relevant reactions require elevated temperatures attained only at the hotter subduction zones. If the presence of fluids is important to tremor generation (discussed in section 5), then hot subduction zones should possess tremor. If this is true, observations of tremor would be expected at the Mexican subduction zone near Guerrero. The present lack of sufficient seismic instrumentation in this region prevents such signals from being detected.

[53] The Boso and Costa Rica subduction zones have interseismic SSEs that locate at relatively shallow depths within their seismogenic zones. At Boso, slow slip occurs between 10 and 20 km depth adjacent to a locked patch, which is speculated to be the possible location of a future Kanto earthquake [Sagiya *et al.*, 1995]. In Costa Rica, slow slip occurs at depths between 15 and 25 km, in a region geodetically determined to be freely slipping at the boundary with a strongly coupled segment of the plate interface [Norabuena *et al.*, 2004]. As mentioned above, slow slip nucleation most likely occurs at frictional transitions within the seismogenic zone at depths above where the continental Moho intersects the downgoing plate, which is consistent with the Costa Rica observations.

[54] In northeast Japan, afterslip is very common following great, large, and even moderate-sized earthquakes and locates both within and below the seismogenic zone. However, interseismic SSEs have not been identified anywhere at this margin. As discussed in section 2.1.1, afterslip is believed to take place in velocity strengthening regions, driven by stress concentrations that remain at frictional transitions after earthquakes. Afterslip occurs within the seismogenic zone of northeast Japan, indicating the presence of such frictional transitions; so why does slow slip not nucleate at these shallow transitions? Previous work has established that the seismogenic zone in northeast Japan is extremely heterogeneous in its frictional properties, consisting of both large and small patches with velocity weakening behavior embedded within regions with velocity strengthening behavior [eg., Igarashi *et al.*, 2003; Uchida *et al.*, 2003]. We hypothesize that this extreme degree of frictional heterogeneity prevents large enough expanses of velocity strengthening material from existing to sustain significant slow slip. Numerical simulations by Kuroki *et al.* [2004] showed that slow slip events had large nucleation zones, lending support to this idea. Figure 1b illustrates this concept, showing seismogenic zones with increasing levels of frictional heterogeneity. The large regions of velocity strengthening material (labeled aseismic on Figure 1b) postulated to exist within the Boso and Costa Rica seismogenic zones may host slow slip, while comparable regions are absent within the northeast Japan seismogenic zone. It is also plausible that the large amount of afterslip following earthquakes in northeast Japan relieves nearly all the stress in the velocity strengthening regions of the plate interface, leaving little to be released in SSEs.

[55] Enough well-documented observations of SSEs exist to begin to investigate various scaling relations. Of the parameters listed in Table 1 the moment magnitude (M_w), which is based on the equivalent seismic moment (M_o), and the source duration (τ) are probably best determined from modeling studies. Seismic moment and earthquake source duration follow the scaling relation $M_o \propto \tau^3$, which implies that earthquake stress drops are constant [Kanamori and Brodsky, 2004]. Figure 9 shows that equivalent seismic moment and source duration scale for interseismic slow

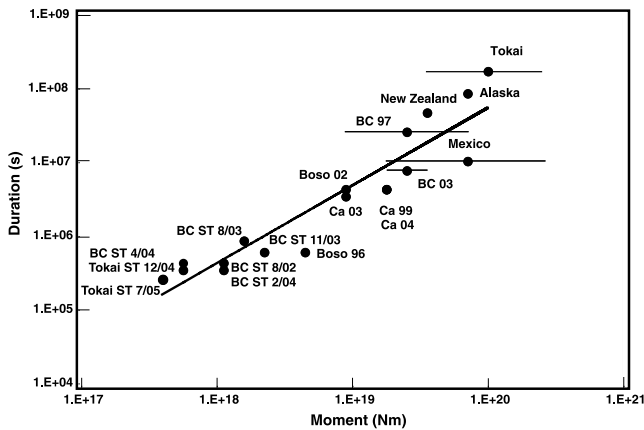


Figure 9. Seismic moment (M_o) and associated uncertainties (horizontal bars) versus duration (τ) scaling relation for slow slip events. SSEs follow the relation $M_o \propto \tau$ as indicated by the best fit line through the data with slope of 1.06. Events are labeled with their location or location and date of occurrence as listed in Table 1. Ca is Cascadia, BC is Bungo Channel, and ST is short-term SSEs.

slip events as well but follow the relation $M_o \propto \tau$, differentiating them from normal earthquakes. Well-characterized afterslip falls off this relationship and, in general, has shorter durations for equivalent seismic moments.

4. SLOW SLIP EVENTS, SEISMICITY, AND TRIGGERING

4.1. Slow Slip and Seismicity in Subduction Zones

[56] Afterslip associated with moderate to large earthquakes suggests a relationship between slow slip and higher-velocity rupture. In addition, models of slow slip generation that appeal to small perturbations in the stress field [e.g., Shen *et al.*, 2005] imply that minute stress changes related to nearby earthquakes could trigger slow slip. Conversely, one of the motivations behind increased study of interseismic slow slip events is the potential triggering effect these events may have for normal earthquakes. Although isolated episodes of interseismic slow slip have been tied to nearby earthquake activity, suggesting a triggering relationship, a pattern has yet to emerge. In an effort to assess whether a consistent pattern exists we plotted the cumulative number of earthquakes within boxes of different sizes encompassing recent SSEs and their cumulative moment scaled by distance cubed from a point in the center of inferred slip. These methods have been used by other authors to assess the seismic response to slow slip for specific SSEs [e.g., Brown *et al.*, 2005; Yamamoto *et al.*, 2005]. We limit our analyses in each region to earthquakes above the completeness threshold for local catalogs (which vary by location). Figure 10 shows analyses for six regions, with plots of the cumulative number of earthquakes between 0 and 60 km depth and the cumulative scaled moment for earthquakes at all depths. We explored a variety of depth ranges and box sizes, and trends do change on the basis of the specific box or point used to compute distances for

cumulative moment scaling. More sophisticated work is clearly warranted, but this exercise strongly indicates that a consistent cause-and-effect relationship does not exist between local, moderate to large seismicity and slow slip events. In the rest of section 4.1 we summarize known associations between seismicity and slow slip activity for each region and suggest some areas for increased study.

4.1.1. Cascadia

[57] In Cascadia, reports of seismicity variations with ETS events are essentially nonexistent, largely because of the limited seismicity in the region. Simple analyses of cumulative moment and number of earthquakes do not reveal any correlation between seismicity and the occurrence of SSEs. Figure 10a shows a plot of cumulative number of earthquakes and scaled cumulative moment using the modeled source region for the February 2002 SSE [Dragert *et al.*, 2004]. The largest earthquake ($M = 4.1$) during 2002 occurred in September, well after the SSE marked by the arrow. The only anomalous rise in earthquake rate occurs in conjunction with this earthquake. In July 2004, two $M > 5$ crustal earthquakes occurred at the beginning of the ETS event. However, this appears to be the only time that large earthquakes are closely associated with ETS activity. An analysis of crustal seismicity rates in the northern Puget Lowlands revealed a periodicity that overlapped the ~ 15 month ETS cyclicity; however, the peaks in seismicity occurred between rather than coincident with the ETS events [Pratt, 2006]. This suggests that a single or set of processes may influence the timing of both ETS and seismicity rather than ETS and seismicity having a direct triggering relationship.

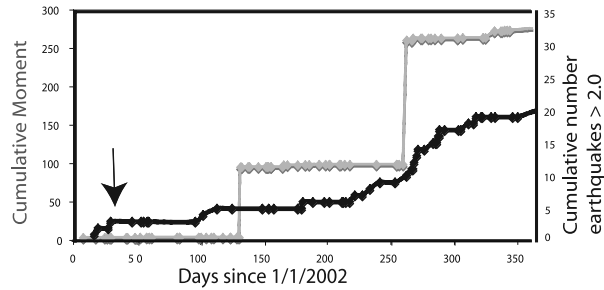
4.1.2. Japan

4.1.2.1. Shikoku

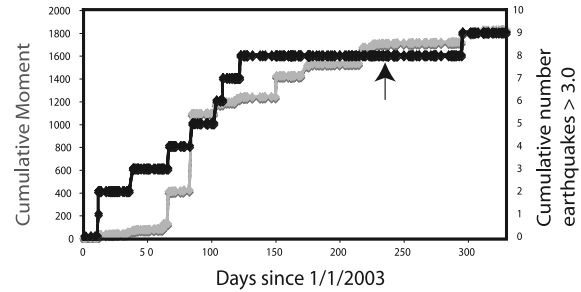
[58] As discussed in section 3.3.2.1, the 1996–1997 slow slip episode may have been affected by changes in stress due to two Hyuganada earthquakes [Hirose *et al.*, 1999], but detailed modeling of slip suggested that interseismic slip in western Shikoku was isolated from the patches of afterslip from these events [Ozawa *et al.*, 2003; Miyazaki *et al.*, 2003]. Additionally, a small swarm of earthquakes (maximum $M_{jma} = 4.9$) occurred north of Bungo Channel in April 1997, just after the initiation of slip [Hirose *et al.*, 1999; Miyazaki *et al.*, 2003]. Most of these events exhibit normal mechanisms and likely occurred in the subducting plate. A similar pattern of nearby earthquakes is not apparent before or during the 2003 slow slip event (Figure 10b). It is possible that stress perturbation caused by the Hyuganada events contributed to the longer duration and larger moment release of the 1996–1997 SSE, but this possibility is difficult to constrain.

[59] In southwest Japan the JMA catalog is complete at least to $M = 2$, making analysis of microroseismicity patterns possible. However, such analyses are complicated by the occurrence of low-frequency earthquakes. These small-magnitude arrivals are included in the JMA catalog but flagged because of their depressed frequency content. In southwest Japan, locations for LFE are roughly consistent with tremor sources, and identified LFE are generally

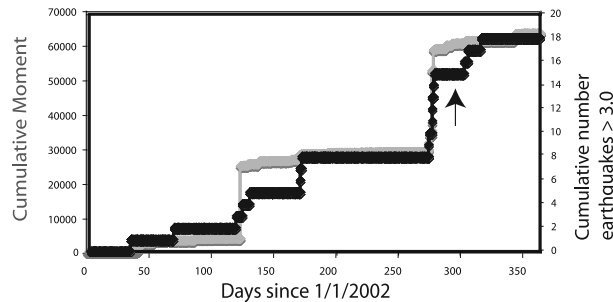
A. Cascadia (February 2002 event)



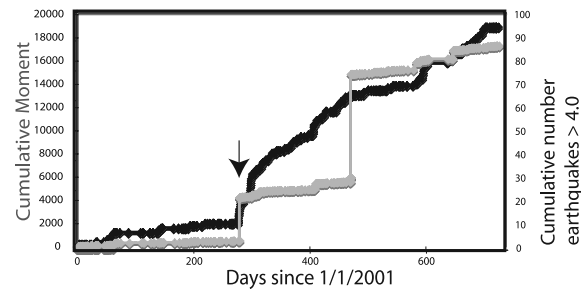
B. Western Shikoku (August 2003 event)



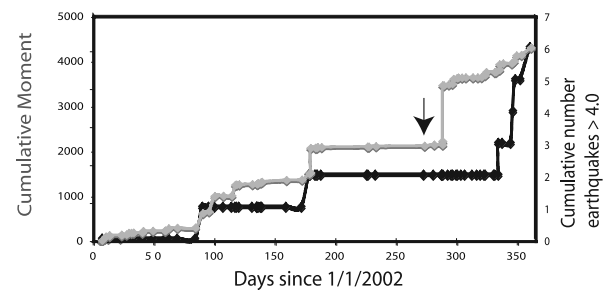
C. Boso (October 2002 event)



D. Mexico (2001-2 event)



E. New Zealand (October 2002 event)



F. Costa Rica (September 2003 event)

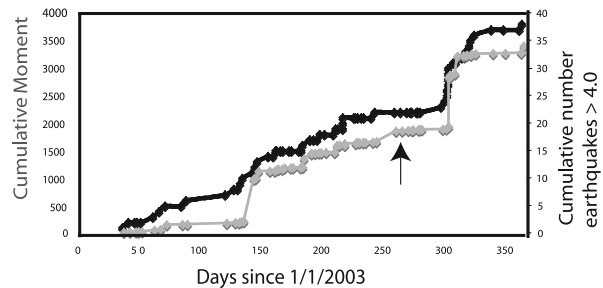


Figure 10. Cumulative number of earthquakes between 0 and 60 km depth occurring within a window around slow slip events (black line) and the cumulative moment of events at all depths scaled by their distance cubed to the middle of the best determined SSE fault plane (gray lines) in six regions. The arrows mark the occurrence of a slow slip event in each region. For earthquakes with no moment magnitude calculated we used the best alternative magnitude to estimate seismic moment. Windows used in the analysis are as follows: (a) 47.3° – 49.3° by -124.5° to -122.5° , (b) 33° – 34° by 132° – 133° , (c) 34.8° – 35.8° by 140° – 141° , (d) 17° – 19° by -101° to -97° , (e) -38.3° to -39.3° by 178.9° – 179.9° , and (f) 8° – 11° by 85° – 87° .

embedded in tremor envelopes. Whether LFEs are a separate but correlated phenomena or whether they are simply the more impulsive end-member of tremor activity remains to be established. When LFE arrivals are removed from the JMA catalog, there does not appear to be any anomalous elevation in microseismicity during active tremor periods in western Shikoku.

4.1.2.2. Tokai

[60] The most extensive work on seismicity patterns and slow slip has been performed for the multiyear Tokai SSE. Volcanism and associated earthquake swarms occurred at nearby Miyake-jima in early June 2000, which was initially thought to precede slow slip. However, recent detailed work suggests that slip precedes this activity [Miyazaki *et al.*,

2006]; nonetheless, a feedback between the two events cannot be ruled out.

[61] Several authors have reported a relative quiescence in shallow (<50 km) seismicity prior to slip in Tokai [Yamamoto *et al.*, 2005; Matsumura, 2006], which could indicate some form of precursory behavior. During the slow slip event, Yoshida *et al.* [2006] reported variations in slab and crustal seismicity concurrent with changes in slip velocity. The rate of slab earthquakes ($M_{jma} > 1.1$) increased in fall 2000 at the initiation of slow slip, decreased in fall 2001 during a period of decreased slip, and rose again in early 2003, coincident with an increase in slip. In contrast, crustal earthquakes experience a relative quiescence in fall 2000 and increase in fall 2001 with decreased slow slip. In

early 2003 the rate of crustal earthquakes rose again, in concurrence with the increase in slab earthquakes and slow slip rate. *Yoshida et al.* [2006] suggested that this pattern of crustal seismicity was related to changes in interplate coupling, with stress increasing during times of increased coupling. In contrast, they suggested that weakened coupling results in increased curvature of the slab as it subducts, which heightens seismicity in the slab. In the context of this relationship the increase in crustal seismicity with accelerated slip in early 2003 is surprising. *Yoshida et al.* [2006] suggested that this change is related to an increase in shortening rate observed in the nearby Suruga Trough, which could increase compressive stress in the crust while promoting acceleration of slow slip deeper on the plate interface. Although this relationship remains preliminary, it is significant as the best documented correlation between seismicity and slow slip. The fact that this correlation is made using seismicity down to $M_{jma} = 1.1$ suggests that a more complete catalog may be necessary for tracking any subtle changes in seismicity resulting from slow slip.

[62] It is also notable that an increase in volcanic low-frequency earthquake activity occurred beneath Mount Fuji during fall 2000 concurrently with increased slab seismicity and slip acceleration. *Yoshida et al.* [2006] suggested that an observed extensional field in and around Mount Fuji may have resulted from increased slip in Tokai. This dilatation may have promoted degassing from a magma body at depth, resulting in the volcanic LFE activity.

4.1.2.3. Boso

[63] *Ozawa et al.* [2003] noted a seismic swarm off the coast of Boso Peninsula on the upper surface of the Philippine Sea plate (20–30 km) concurrent with the 2002 slow slip event. This increased activity is quite apparent in Figure 10c. A similar swarm occurred during the 1996 slow slip event, suggesting a consistent relationship between microseismicity and slow slip [*Sagiya, 2004*]. *Ozawa et al.* [2003] suggested that this swarm activity increased stress in the neighboring region and caused the observed slow slip. Consequently, these authors used other peaks in seismicity to propose additional slip events in 1983 and 1991–1992 (consistent with the inferred 6–7 year recurrence interval).

4.1.3. Mexico

[64] *Lowry et al.* [2001] reported enhanced seismicity up dip of the 1998 slip event during the months following it, but the timing makes it unlikely that there is a direct connection. For the largest SSE in 2001, *Kostoglodov et al.* [2003] reported two “unusual” shallow earthquakes that bookend the slow event. A normal faulting earthquake occurred in the crust on 8 October 2001 ($M_w = 5.9$), and a particularly large $M_w = 6.7$ tsunamigenic earthquake occurred near the trench on 18 April 2002. The former produced significant aftershocks in the region, which elevated seismicity rates during the beginning of the SSE (Figure 10d). Plausibly, the magnitude of the 2001–2002 event was enhanced by the concurrent aftershock activity. The increased stress perturbations from this large event likely acted as a more effective trigger for large earthquakes

by bringing the asperity of the 18 April event closer to failure. Given the magnitude of the 2001–2002 event relative to other Mexico slow slip events, it is difficult to assess whether the correlation between these two events is a consistent feature of aseismic slip in Guerrero. Simple cumulative moment and earthquake plots for other Guerrero SSEs do not reveal a consistent pattern of triggering; however, more rigorous work should be done to track seismicity rates in the region as subtle patterns may emerge.

4.1.4. New Zealand

[65] The interpretation also remains ambiguous for New Zealand. Near the end of the 2002 SSE a shallow magnitude 4.9 earthquake occurred offshore of the North Island outside the slow slip source area, which accounts for a peak in scaled moment release. An additional jump in moment release occurred in late June (a 4.8 earthquake offshore), well before the initiation of slow slip (Figure 10e). Simple catalog analyses also suggest a peak in earthquakes between 30 and 60 km about a month after the cessation of slow slip in 2002. Any of this activity could be related to slow slip, but this possibility is tempered given that this behavior is not particularly anomalous and that similar behavior is not apparent for the 2004 event.

4.1.5. Costa Rica

[66] *Brown et al.* [2005] reported a rise in moment release 20 days after each 2000 fluid flow event. In addition, a series of earthquakes occurred near the trench in July 2000, following the final fluid flow event. Despite the lag time, there may be a connection between this activity and stress perturbations induced by slow slip, as suggested by the authors.

[67] A series of events northwest of the slow slip focus occurred in late October 2003, at the end of the 2003 event (Figure 10f). These events may have been triggered by slow slip, but given uncertainties in modeled slip area, the strength of this connection remains quite uncertain.

4.2. Relationship Between SSEs and Microseismicity in Nonsubduction Regions

[68] Because it is suggested that stress perturbations from large earthquakes and slow slip trigger tremor, one might expect microseismicity to follow suit. In Hawaii, microseismicity appears to follow a characteristic aftershock distribution in modeled regions of positive stress perturbation caused by slow slip, and it also appears to follow a characteristic aftershock distribution [*Segall et al., 2006*]. This behavior strongly suggests that static stress changes induced by slow slip are capable of perturbing seismicity, but as *Segall et al.* [2006] suggest, this behavior may be difficult to detect in regions with low levels of background seismicity (e.g., Cascadia).

[69] Additionally, the correlation between earthquake rates and tremor activity in the San Andreas Fault [*Nadeau and Dolenc, 2005*] suggests the possibility that tremor in subduction zones somehow harkens an increase in normal seismicity. However, there does not appear to be a consistent relationship between the number of small earthquakes and tremor activity. Lack of catalog completeness is clearly

a hindrance to such analyses, especially given that correlation for the San Andreas Fault was made for earthquakes with $M_w < 2.1$, which is below the completeness threshold of most catalogs.

4.3. Implications

[70] Earthquakes clearly trigger slower slip, as demonstrated by afterslip immediately following moderate to large earthquakes. However, the connection between interseismic slip and earthquake activity is less apparent, considering the spectrum of behavior reported (e.g., quiescence, potentially SSE-triggering earthquakes, and apparent SSE-triggered seismicity). This result may not be surprising given the apparent complexity of normal earthquake triggering [Freed, 2005].

[71] The correlation between increased microseismicity and slow slip in nonsubduction regions (section 4.2) suggests that slow slip may be effective at triggering small earthquakes. In Tokai, where catalog completeness allows similar analyses, a correlation is found between earthquake activity in the downgoing slab and overlying crust and acceleration and deceleration of slow slip, but the relationship is apparently complex. Increased catalog completeness and the use of more sophisticated methodologies will help illuminate how consistently slow slip perturbs microseismicity in the slab and overlying crust.

[72] Although it is difficult to constrain, dynamic stresses induced by distant earthquakes could affect slip activity. Work on remote triggering suggests that shaking as low as 0.2 cm/s induced by passing teleseismic waves can trigger earthquakes [Prejean *et al.*, 2004]. In the current absence of similar work applied to slow slip we do not address this possibility here. However, statistical techniques employed to test remote triggering of earthquakes [e.g., Brodsky *et al.*, 2000; Harrington and Brodsky, 2006] should be applied to assess this possibility.

5. MECHANISMS

5.1. Triggering of Slow Slip Events

[73] Although fluids have been implicated in most proposed tremor-generating mechanisms, their direct involvement in the initiation of slow slip is still questionable. Kodaira *et al.* [2004] attributed slow slip in the Tokai, Japan, region to elevated fluid pressure that extended the width of the frictional transition zone where slow slip is generated. Several numerical modeling studies involving rate- and state-dependent friction show that slow slip events require spatial or temporal variations in frictional properties that cause heterogeneous stress distributions but not time-dependent pore pressures expected from fluid release [Yoshida and Kato, 2003; Kuroki *et al.*, 2004; Liu and Rice, 2005]. It is fairly well established that slow slip events initiate at transitions in frictional properties from unstable to stable sliding where the occurrence of nearby large earthquakes produce stress and slip heterogeneities along the plate interface. What triggers SSEs is much less well understood. Section 4.1 evaluated evidence for seismic

triggering of SSEs; here we discuss other phenomena that have been suggested as triggering sources for SSEs.

[74] Most SSEs are recurrent, with repeat intervals that range from many years (long-term SSEs in the Bungo Channel, Boso, and possibly Tokai, Japan) to a few months (short-term SSEs in southwest Japan). The recurrence interval for SSEs in northern Cascadia is well established at 13–16 months. Miller *et al.* [2002] noted that this repeat interval encompasses the 14.5 month periodicity of the Earth's Chandler wobble (wobble of Earth's rotation axis caused by mass redistribution at the Earth's surface) but dismissed a causative relationship because of the small size of the stress perturbations generated. Shen *et al.* [2005] quantitatively investigated this relationship by calculating the stress changes induced by the Chandler wobble near the frictional transition zone of the plate interface in northern and southern Cascadia; Guerrero, Mexico; Bungo Channel; and Boso Peninsula, Japan, and comparing them with SSE cyclicity. They found that 14 out of 20 SSEs occurred just prior to and 3 occurred synchronous with induced stress changes attaining their maxima. They concluded that although these stress perturbations were very small (between 0.2 and 1 kPa), the long period (14.5 months) of the modulating stress was critical in reducing the triggering threshold and inducing slow slip. The triggered events were SSEs rather than earthquakes because the triggering threshold is lowered in the region of the fault plane with frictional conditions that favor SSEs.

[75] Lowry [2006] hypothesized that periodic slow slip is a resonant fault response to stress perturbations caused by the Chandler wobble and/or other climatic loading phenomena. However, he found that on average, hydrologic stress perturbations are at least a factor of two greater than those generated by the Chandler wobble. He noted that for slip to be triggered by hydrologic or other climatic forcing it must respond preferentially to longer period stress oscillations. Perfettini and Schmittbuhl [2001] found that slip resulting from an applied stress was amplified provided that the frictional conditions were near the stability transition and the period of loading was close to a critical value. Lowry [2006] called this critical period for slip amplification the natural resonant period of the fault and showed that it depended on frictional parameters of the fault plane and the plate convergence velocity. He speculated that environmental loading by the ocean, atmosphere, and tides provided a broad enough spectrum of forcing signals to potentially match the resonant periods of all fault planes hosting SSEs.

5.2. Tremor Generation Models

[76] On the basis of the spectral properties of subduction tremor and its presumed similarity to volcanic tremor most models for tremor nucleation invoke the presence of fluids. The evidence for such a connection is strong. Tremor sources in southwest Japan and Cascadia are roughly consistent with the expected region in which fluid is expelled from the dehydration of minerals (e.g., chlorite and amphibole) in the subducting slab [Katsumata and Kamaya, 2003]. In addition, others [e.g., Seno and Yama-

saki, 2003] have argued that the absence of tremor in regions of southwest Japan where island arc type crust (with low water content) subducts suggests that the dehydration of fluids from the crust of the subducting slab is an important controlling factor in tremor generation. As mentioned in sections 3.3.1 and 3.3.2, the clustering of tremor sources around inferred regions of high fluid content, inferred from V_p/V_s ratios, further strengthens this connection. Although early work emphasized the similarity between subduction and volcanic tremor in proposing resonance mechanisms, the lack of any harmonic character to subduction tremor makes such a mechanism unlikely. Instead, it seems more likely that tremor reflects some sort of shear failure. The weakening of rock material due to increased fluid content and/or fracturing could depress the frequency content of released energy. Analyses of moveout curves for tremor bursts suggest that multiple sources are active at the same time [McCausland *et al.*, 2005]. This result provides some additional evidence for a model in which multiple sources of shear failure interfere to create an emergent and long-duration tremor signal. Recent work establishing the linear distribution of LFEs on or near the plate interface beneath Shikoku, Japan, and demonstrating the similarity between these LFEs and tremor [Shelly *et al.*, 2006, 2007] clearly demonstrates that some tremor is generated by swarms of earthquakes in response to plate motions. The discovery of very low frequency earthquakes, with reverse faulting mechanisms, temporally and spatially coincident with tremor and LFEs in southwest Japan [Ito *et al.*, 2006] corroborates this interpretation.

[77] Given their correspondence, proposed mechanisms for tremor generally hinge on the relationship between slow slip and tremor. Three main possibilities exist: (1) slow slip and tremor are manifestations of the same phenomena, (2) slow slip triggers tremor activity in regions with particular characteristics, or (3) tremor and slow slip are both independently triggered by some other phenomena.

[78] In the first category some researchers suggested that tremor may represent patches of more accelerated shear failure on the plate interface surrounded by broad regions of slow slip [Shelly *et al.*, 2006; Ito *et al.*, 2006]. However, the wide distribution apparent in Cascadia argues against slip on the plate interface as a dominant mechanism for tremor, at least in this region. Alternatively, such a mechanism may account for the more impulsive end-member of low-frequency seismic behavior (so-called LFEs and VLFEs) observed in southwest Japan, while some other mechanism causes the long-duration tremor in which they are embedded.

[79] It is also plausible that some outside force serves to trigger both slip and tremor activity (category 3). Potential triggers of slip are outlined in more detail in section 5.1, but for the purposes of this discussion the most relevant suggestion is that fluid outflows from the slab could lubricate the fault surface and increase pore pressure, promoting slip [e.g., Melbourne and Webb, 2003]. This rapid fluid flow could also trigger tremor activity as it dissipates in the overriding crust (e.g., through the promo-

tion of microfracturing). Although it is difficult to rule this mechanism out, it is not clear what would cause defined “bursts” of fluids. Especially in light of the apparent triggering of tremor by teleseismic earthquakes, what seems more likely is that tremor is triggered by the stress perturbation imparted by slow slip (category 2). Kao *et al.* [2006] show that for a slip model with the same parameterization used by Dragert *et al.* [2001] the majority of tremor occurs in positive dilatational quadrants. The correlation between tremor and dilatational strain and fluids is similar to the mechanism proposed by Miyazawa and Mori [2006] for tremor/LFE triggered by teleseismic earthquakes. Volumetric changes could promote the movement of fluids into cracks, which would reduce frictional stress, promoting fracture and brittle failure. One limitation to this proposed mechanism is the observation that tremor sometimes precedes GPS- or tiltmeter-resolved slip by several days [Obara and Hirose, 2006]. However, the initiation of slow slip is difficult to resolve, and early tremor may be triggered by slip that is below the resolution of current instrumentation. More detailed processing of the GPS record may clarify the relative timing of tremor peaks and slow slip initiation and cessation, which will help in assessing the possibility that slow slip directly triggers tremor. In addition, tracking the correspondence between expected strain perturbations from slip and tremor locations in a variety of regions would aid in the continued evaluation of this mechanism.

6. FUTURE DIRECTIONS

[80] Aseismic transient slip has been identified at most plate boundaries where continuous long-period instrumentation capable of detecting slow deformation exists. In fact, the scarcity of historically reported transients is most likely a consequence of the inability to observe them, rather than their absence. The Plate Boundary Observatory (PBO) component of Earthscope, established to study the strain field resulting from active deformation between the Pacific and North American plates, is well poised to remedy this situation in western North America. PBO is in the process of deploying a dense array of continuously operating GPS receivers and strainmeters in the western United States favorably positioned to record strain transients associated with the Cascadia and Alaskan subduction zones and the San Andreas Fault. Geodetic data collected at PBO stations with stable monumentation and long time series promise to be useful in improving our understanding of slow slip events at these locations. Parallel efforts are under way to expand sparse GPS networks in regions that have already recorded SSEs. For example, a 12-station network of continuous GPS stations is presently under construction on the Nicoya Peninsula in northern Costa Rica, and the Institute of Geological and Nuclear Sciences in New Zealand plans to install 10–20 continuous GPS stations each year through about 2010 as part of the GEONET project.

[81] Progress in developing and using other geodetic techniques capable of detecting and studying slow slip

events at plate boundaries is also being made. For example, Lambert *et al.* [2006] demonstrated that terrestrial absolute gravity measurements can be used in conjunction with space-based measurements to detect short-term gravity variations associated with slow slip events. Researchers at Central Washington University and University of Colorado are installing biaxial Michelson tiltmeters near Seattle, Washington, to monitor surface tilts associated with the northern Cascadia slow slip events (see <http://www.geodesy.cwu.edu>). A similar long-baseline tiltmeter was installed in Guerrero, Mexico [Kostoglodov *et al.*, 2002]. Long-baseline tiltmeter data complement GPS data by providing higher precision. Many more efforts in the future to establish and upgrade monitoring capabilities at active plate boundaries will undoubtedly contribute to a fast growing database of SSEs to study, resulting in new revelations about this fascinating phenomena.

7. CONCLUSIONS

[82] The increasing density of continuous GPS observations worldwide has revealed slow slip to be a ubiquitous process that constitutes a fundamental mode of strain release at plate boundaries. For a long time the aseismic component of plate motions has been assumed to take place primarily as steady state creep, although no direct observations of creep at depth exist. This paper summarizes the accumulating evidence to support a model where a large fraction of aseismic slip at subduction zones occurs episodically in slow slip events rather than continuously. These slow slip events appear to have a significant influence on other, probably interrelated, tectonic processes such as pore fluid pressurization and expulsion at the seafloor and earthquake nucleation. It is too early in the study of aseismic strain transients to make grandiose conclusions about their behavior; however, it is certain that continued study of these phenomena is critical to attaining a meaningful understanding of seismogenic zones.

[83] **ACKNOWLEDGMENTS.** We thank Kazushige Obara, Wendy McCausland, and Chloe Peterson for sending us tremor waveforms from Japan, Cascadia, and Alaska. We are grateful to Kazushige Obara, David Shelly, Jeff Freymueller, Michael Brudzinski, Tony Lowry, and John Beavan for providing copies of their papers prior to publication, to Greg Beroza for providing stacked tremor spectra from SW Japan used in Figure 5a, and to Steve Malone for sharing his tremor processing algorithm with us. We thank Tim Dixon and Emily Brodsky for enlightening conversations about slow slip events and Kelin Wang and Tim Melbourne for providing thorough and critical reviews of an earlier version of this manuscript that greatly improved it. This work was supported by NSF through award EAR-0506463 to SYS.

[84] The Editor responsible for this paper was Michael Manga. He thanks technical reviewers Tim Melbourne and Kelin Wang.

REFERENCES

- Aguiar, A. C., T. I. Melbourne, and C. W. Scrivner (2006), Automated tremor analysis from the Cascadia subduction zone, *Eos Trans. AGU*, 87(52), Fall Meet. Suppl., Abstract T41A-1536.
- Ando, M. (1975), Source mechanisms and tectonic significance of historical earthquakes along the Nankai Trough, Japan, *Tectonophysics*, 27, 119–140.
- Beavan, J., L. Wallace, A. Douglas, H. Fletcher, and J. Townend (2007), Slow slip events on the Hikurangi subduction interface, New Zealand, in *Dynamic Planet: Monitoring and Understanding a Dynamic Planet with Geodetic and Oceanographic Tools: IAG Symposium, Cairns, Australia, 22–26 August 2005*, *Int. Assoc. Geod. Symp.*, vol. 130, edited by P. Tregoning and C. Rizos, pp. 438–444, Springer, New York.
- Beroza, G. C., and T. Jordan (1990), Searching for slow and silent earthquakes, *J. Geophys. Res.*, 95, 2485–2510.
- Bilek, S. L., T. Lay, and L. J. Ruff (2004), Radiated seismic energy and earthquake source duration variations from teleseismic source time functions for shallow subduction zone thrust earthquakes, *J. Geophys. Res.*, 109, B09308, doi:10.1029/2004JB003039.
- Boettcher, M. S., and T. H. Jordan (2004), Earthquake scaling relations for mid-ocean ridge transform faults, *J. Geophys. Res.*, 109, B12302, doi:10.1029/2004JB003110.
- Brodsky, E. E., V. Karakostas, and H. Kanamori (2000), A new observation of dynamically triggered regional seismicity: Earthquakes in Greece following the August 1999 Izmit, Turkey earthquake, *Geophys. Res. Lett.*, 27, 2741–2744.
- Brooks, B. A., J. H. Foster, M. Bevis, L. N. Frazer, C. J. Wolfe, and M. Behn (2006), Periodic slow earthquakes on the flank of Kilauea volcano, Hawaii, *Earth Planet. Sci. Lett.*, 246, 207–216.
- Brown, K. M., M. D. Tryon, H. R. DeShon, L. M. Dorman, and S. Y. Schwartz (2005), Correlated transient fluid pulsing and seismic tremor in the Costa Rica subduction zone, *Earth Planet. Sci. Lett.*, 238, 189–203.
- Brudzinski, M. R., and R. Allen (2006), Segmentation in episodic tremor and slip all along Cascadia, *Eos Trans. AGU*, 87(52), Fall Meet. Suppl., Abstract T53G-05.
- Bucknam, R. C., G. Plafker, and R. V. Sharp (1978), Fault movement (afterslip) following the Guatemala earthquake of February 4, 1976, *Geology*, 6, 170–173.
- Bürgmann, R., D. Schmidt, R. M. Nadeau, M. d'Alessio, E. Fielding, D. Manaker, T. V. McEvilly, and M. H. Murray (2000), Earthquake potential along the northern Hayward Fault, California, *Science*, 289, 1178–1182.
- Bürgmann, R., M. G. Kogan, V. E. Levin, C. H. Scholz, R. W. King, and G. M. Steblov (2001), Rapid aseismic moment release following the 5 December 1997 Kronotsky Kamchatka earthquake, *Geophys. Res. Lett.*, 28, 1331–1334.
- Cervelli, P., P. Segall, K. Johnson, M. Lisowski, and A. Miklius (2002), Sudden aseismic fault slip on the south flank of Kilauea volcano, *Nature*, 415, 1014–1018.
- Cohen, S. C., and J. T. Freymueller (2004), Crustal deformation in southcentral Alaska subduction zone: The 1964 Prince William Sound earthquake, *Adv. Geophys.*, 47, 1–63.
- Davis, E. E., K. Becker, K. Wang, K. Obara, Y. Ito, and M. Kinoshita (2006), A discrete episode of seismic and aseismic deformation of the Nankai trough subduction zone accretionary prism and incoming Philippine Sea plate, *Earth Planet. Sci. Lett.*, 242, 73–84.
- Delahaye, E. J., J. Townend, M. E. Reyners, and M. P. Chadwick (2006), Seismic tremor and small earthquakes associated with slow slip in the Hikurangi subduction zone, New Zealand, *Eos Trans. AGU*, 87(52), Fall Meet. Suppl., Abstract T41A-1548.
- DeMets, C. (2001), A new estimate for Cocos-Caribbean plate motion: Implications for slip along the Central American volcanic arc, *Geophys. Res. Lett.*, 28, 4043–4046.
- Douglas, A., J. Beavan, L. Wallace, and J. Townend (2005), Slow slip on the northern Hikurangi subduction interface, New Zealand, *Geophys. Res. Lett.*, 32, L16305, doi:10.1029/2005GL023607.
- Dragert, H., K. Wang, and T. S. James (2001), A silent slip event on the deeper Cascadia subduction interface, *Science*, 292, 1525–1528.

- Dragert, H., K. Wang, and G. Rogers (2004), Geodetic and seismic signatures of episodic tremor and slip in the northern Cascadia subduction zone, *Earth Planets Space*, *56*, 1143–1150.
- Franco, S. I., V. Kostoglodov, K. M. Larsen, V. C. Manea, M. Manea, and J. A. Santiago (2005), Propagation of the 2001–2002 silent earthquake and interplate coupling in the Oaxaca subduction zone, Mexico, *Earth Planets Space*, *57*, 973–985.
- Freed, A. M. (2005), Earthquake triggering by static, dynamic and postseismic stress transfer, *Annu. Rev. Earth Planet. Sci.*, *33*, 335–367.
- Frey Mueller, J. T., S. Hreinsdóttir, C. Zweck, and P. J. Haeussler (2002), The 1998–2002 deep megathrust slip event, Alaska, *Eos Trans. AGU*, *83*(47), Fall Meet. Suppl., Abstract G61A-0972.
- Galehouse, J. S. (2002), Data from theodolite measurements of creep rates on San Francisco Bay Region faults, California: 1979–2001, *U.S. Geol. Surv. Open File Rep.*, *02-225*.
- Gao, H., and D. A. Schmidt (2006), The slip history of the 2004 slow slip event on the northern Cascadia subduction zone, *Eos Trans. AGU*, *87*(52), Fall Meet. Suppl., Abstract T41A-1540.
- Gao, S. S., P. G. Silver, and A. T. Linde (2000), Analysis of deformation data at Parkfield, California: Detection of a long-term strain transient, *J. Geophys. Res.*, *105*, 2955–2968.
- Gladwin, M. T. (2004), Maintenance, data archive and analysis of existing low-frequency GTSM installations in California, National Earthquake Hazard Reduction Program annual project summary, U.S. Geol. Surv., Reston, Va.
- Gwyther, R. L., C. H. Thurber, M. T. Gladwin, and M. Mee (2000), Seismic and aseismic observations of the 12th August 1998 San Juan Bautista, California $M_{5.3}$ earthquake, paper presented at 3rd Conference on Tectonic Problems of the San Andreas Fault System, Stanford Univ., Stanford, Calif.
- Harrington, R. M., and E. E. Brodsky (2006), The absence of remotely triggered seismicity in Japan, *Bull. Seismol. Soc. Am.*, *96*, 871–878.
- Hearn, E. H. (2003), What can GPS tell us about the dynamics of post-seismic deformation?, *Geophys. J. Int.*, *155*, 753–777.
- Heki, K., S. Miyazaki, and H. Tsuji (1997), Silent fault slip following an interplate thrust earthquake at the Japan Trench, *Nature*, *386*, 595–598.
- Hirose, H., and K. Obara (2005), Repeating short- and long-term slow slip events with deep tremor activity around the Bungo Channel region, southwest Japan, *Earth Planets Space*, *57*, 961–972.
- Hirose, H., and K. Obara (2006), Short-term slow slip and correlated tremor episodes in the Tokai region, central Japan, *Geophys. Res. Lett.*, *33*, L17311, doi:10.1029/2006GL026579.
- Hirose, H., K. Hirahara, F. Kimata, N. Fujii, and S. Miyazaki (1999), A slow thrust slip event following the two 1996 Hyuganada earthquakes beneath the Bungo Channel, southwest Japan, *Geophys. Res. Lett.*, *26*, 3237–3240.
- Hsu, Y.-J., M. Simons, J.-P. Avouac, J. Galetzka, K. Sieh, M. Chlieh, D. Natawidjaja, L. Prawirodirdjo, and Y. Bock (2006), Frictional afterslip following the 2005 Nias-Simeulue earthquake, Sumatra, *Science*, *312*, 1921–1926.
- Hutton, W., C. DeMets, O. Sanchez, G. Suarez, and J. Stock (2001), Slip kinematics and dynamics during and after the 1995 October 9 $M_w = 8.0$ Colima-Jalisco earthquake, Mexico, from GPS geodetic constraints, *Geophys. J. Int.*, *146*, 637–658.
- Hyndman, R. D., K. Wang, and M. Yamano (1995), Thermal constraints on the seismogenic portion of the southwestern Japan subduction thrust, *J. Geophys. Res.*, *100*, 15,373–15,392.
- Igarashi, T., T. Matsuzawa, and A. Hasegawa (2003), Repeating earthquakes and interplate aseismic slip in the northeastern Japan subduction zone, *J. Geophys. Res.*, *108*(B5), 2249, doi:10.1029/2002JB001920.
- Iinuma, T., M. Protti, K. Obana, V. Gonzalez, R. van der Laat, T. Kato, S. Miyasaki, Y. Kaneda, and E. Hernandez (2004), Interplate coupling in the Nicoya Peninsula, Costa Rica, as deduced from a trans-peninsula GPS experiment, *Earth Planet. Sci. Lett.*, *223*, 203–212.
- Ito, T., and M. Hashimoto (2004), Spatiotemporal distribution of interplate coupling in southwest Japan from inversion of geodetic data, *J. Geophys. Res.*, *109*, B02315, doi:10.1029/2002JB002358.
- Ito, Y., and K. Obara (2006a), Dynamic deformation of the accretionary prism excites very low frequency earthquakes, *Geophys. Res. Lett.*, *33*, L02311, doi:10.1029/2005GL025270.
- Ito, Y., and K. Obara (2006B), Very low frequency earthquakes within accretionary prisms are very low stress-drop earthquakes, *Geophys. Res. Lett.*, *33*, L09302, doi:10.1029/2006GL025883.
- Ito, T., S. Yoshioka, and S. Miyazaki (1999), Interplate coupling in southwest Japan deduced from inversion analysis of GPS data, *Phys. Earth Planet. Inter.*, *115*, 17–34.
- Ito, Y., K. Obara, K. Shiomi, S. Sekine, and H. Hirose (2006), Slow earthquakes coincident with episodic tremors and slow slip events, *Science*, *315*, 503–506, doi:10.1126/science.1134454.
- Johnston, M. J. S. (1997), Near-silent earthquakes on the San Andreas Fault system, *Eos Trans. AGU*, *78*(46), Fall Meet. Suppl., F156.
- Johnston, M. J. S., R. L. Gwyther, A. T. Linde, M. T. Gladwin, G. D. Myren, and R. J. Mueller (1996), Another slow earthquake on the San Andreas Fault triggered by a $M_{4.7}$ earthquake on April 19, 1996, *Eos Trans. AGU*, *77*(46), Fall Meet. Suppl., F515.
- Kanamori, H., and E. E. Brodsky (2004), The physics of earthquakes, *Rep. Prog. Phys.*, *67*, 1429–1496.
- Kanamori, H., and J. Cipar (1974), Focal process of the great Chilean earthquake May 22, 1960, *Phys. Earth Planet. Inter.*, *9*, 127–136.
- Kanamori, H., and M. Kikuchi (1993), The 1992 Nicaragua earthquake: A slow tsunami earthquake associated with subducted sediments, *Nature*, *361*, 714–716.
- Kanamori, H., and G. S. Stewart (1976), Mode of strain release along the Gibbs fracture zone, Mid-Atlantic Ridge, *Phys. Earth Planet. Inter.*, *11*, 312–332.
- Kao, H., S. Shan, H. Dragert, G. Rogers, J. F. Cassidy, and K. Ramachandran (2005), A wide depth distribution of seismic tremors along the northern Cascadia margin, *Nature*, *436*, 841–844.
- Kao, H., S. Shan, H. Dragert, G. Rogers, J. F. Cassidy, K. Wang, T. James, and K. Ramachandran (2006), Spatial-temporal patterns of seismic tremors in northern Cascadia, *J. Geophys. Res.*, *111*, B03309, doi:10.1029/2005JB003727.
- Katsumata, A., and N. Kamaya (2003), Low-frequency continuous tremor around the Moho discontinuity away from volcanoes in the southwest Japan, *Geophys. Res. Lett.*, *30*(1), 1020, doi:10.1029/2002GL015981.
- Kawasaki, I., Y. Asai, Y. Tamura, T. Sagiya, N. Mikami, Y. Okada, M. Sakata, and M. Kasahara (1995), The 1992 Sanriku-Oki, Japan, ultra-slow earthquake, *J. Phys. Earth.*, *43*, 105–116.
- Kawasaki, I., Y. Asai, and Y. Tamura (2001), Space-time distribution of interplate moment release including slow earthquakes and the seismogeodetic coupling in the Sanriku-Oki region along the Japan trench, *Tectonophysics*, *330*, 267–283.
- Kikuchi, M., M. Nakamura, and K. Yoshikawa (2003), Source rupture processes of the 1944 Tonankai earthquake and the 1945 Mikawa earthquake derived from low-gain seismograms, *Earth Planets Space*, *55*, 159–172.
- Kodaira, S., T. Iidaka, A. Kato, J. Park, T. Iwasaki, and Y. Kaneda (2004), High pore fluid pressure may cause silent slip in the Nankai Trough, *Science*, *304*, 1295–1299, doi:10.1126/science.1096535.
- Kostoglodov, V., R. Bilham, J. A. Santiago, V. Manea, M. Manea, and V. R. Hernandez (2002), Long-baseline fluid tiltmeter for seismotectonic studies of Mexican subduction zone, *Geofis. Int.*, *41*, 11–25.
- Kostoglodov, V., S. K. Singh, J. A. Santiago, S. I. Franco, K. M. Larson, A. R. Lowry, and R. Bilham (2003), A large silent earthquake in the Guerrero seismic gap, Mexico, *Geophys. Res. Lett.*, *30*(15), 1807, doi:10.1029/2003GL017219.

- Kreemer, C., G. Blewitt, and F. Maerten (2006), Co- and postseismic deformation of the 28 March 2005 Nias M_w 8.7 earthquake from continuous GPS data, *Geophys. Res. Lett.*, *33*, L07307, doi:10.1029/2005GL025566.
- Kurashimo, E., and H. Naoshi (2004), Low V_p and V_p/V_s zone beneath the northern Fossa Magna basin, central Japan, derived from a dense array observation, *Earth Planets Space*, *56*, 1301–1308.
- Kuroki, H., H. M. Ito, H. Takayama, and A. Yoshida (2004), 3-D simulation of the occurrence of slow slip events in the Tokai region with a rate- and state-dependent friction law, *Bull. Seismol. Soc. Am.*, *94*, 2037–2050.
- Lambert, A., N. Courtier, and T. S. James (2006), Long-term monitoring by absolute gravimetry: Tides to postglacial rebound, *J. Geodyn.*, *41*, 307–317.
- Langbein, J., R. L. Gwyther, R. H. G. Hart, and M. T. Gladwin (1999), Slip-rate increase at Parkfield in 1993 detected by high-precision EDM and borehole tensor strainmeters, *Geophys. Res. Lett.*, *26*, 2529–2532.
- La Rocca, M., W. McCausland, D. Galluzzo, S. Malone, G. Saccorotti, and E. Del Pezzo (2005), Array measurements of deep tremor signals in the Cascadia subduction zone, *Geophys. Res. Lett.*, *32*, L21319, doi:10.1029/2005GL023974.
- Larson, K. M., V. Kostoglodov, A. Lowry, W. Hutton, O. Sanchez, K. Hudnut, and G. Suarez (2004), Crustal deformation measurements in Guerrero, Mexico, *J. Geophys. Res.*, *109*, B04409, doi:10.1029/2003JB002843.
- Linde, A. T., and S. I. Sacks (2002), Slow earthquakes and great earthquakes along the Nankai Trough, *Earth Planet Sci. Lett.*, *203*, 265–275.
- Linde, A. T., and P. G. Silver (1989), Elevation changes and the great 1960 Chilean earthquake: Support for aseismic slip, *Geophys. Res. Lett.*, *16*, 1305–1308.
- Linde, A. T., K. Suyehiro, M. Satoshi, S. I. Sacks, and A. Takagi (1988), Episodic aseismic earthquake precursors, *Nature*, *334*, 513–515.
- Linde, A. T., M. Gladwin, M. Johnston, R. Gwyther, and R. Bilham (1996), A slow earthquake sequence on the San Andreas Fault, *Nature*, *383*, 65–68.
- Liu, Y., and J. R. Rice (2005), Aseismic slip transients emerge spontaneously in three-dimensional rate and state modeling of subduction earthquake sequences, *J. Geophys. Res.*, *110*, B08307, doi:10.1029/2004JB003424.
- Lowry, A. R. (2006), Resonant slow fault slip in subduction zones forced by climatic load stress, *Nature*, *442*, 802–805.
- Lowry, A. R., K. M. Larson, V. Kostoglodov, and R. Bilham (2001), Transient fault slip in Guerrero, southern Mexico, *Geophys. Res. Lett.*, *28*, 3753–3756.
- Lowry, A. R., K. M. Larson, V. Kostoglodov, and O. Sanchez (2005), The fault slip budget in Guerrero, southern Mexico, *Geophys. J. Int.*, *200*, 1–15.
- Lundgren, P., M. Protti, A. Donnellan, M. Heflin, E. Hernandez, and D. Jefferson (1999), Seismic cycle and plate margin deformation in Costa Rica: GPS observations from 1994 to 1997, *J. Geophys. Res.*, *104*, 28,915–28,928.
- Malservisi, R., C. Gans, and K. P. Furlong (2003), Numerical modeling of creeping faults and implications for the Hayward Fault, California, *Tectonophysics*, *361*, 121–137.
- Marone, C. J., C. H. Scholtz, and R. Bilham (1991), On the mechanics of afterslip, *J. Geophys. Res.*, *96*, 8441–8452.
- Matsubara, M., Y. Yagi, and K. Obara (2005), Plate boundary slip associated with the 2003 Off-Tokachi earthquake based on small repeating earthquakes, *Geophys. Res. Lett.*, *32*, L08316, doi:10.1029/2004GL022310.
- Matsumura, S. (2006), Seismic activity changes progressing simultaneously with slow-slip in the Tokai area, *Tectonophysics*, *417*, 5–15.
- McCausland, W., S. Malone, and D. Johnson (2005), Temporal and spatial occurrence of deep non-volcanic tremor: From Washington to northern California, *Geophys. Res. Lett.*, *32*, L24311, doi:10.1029/2005GL024349.
- McGuire, J. J., and P. Segall (2003), Imaging of aseismic fault slip transients recorded by dense geodetic networks, *Geophys. J. Int.*, *155*, 778–788.
- Melbourne, T. I., and F. H. Webb (2002), Precursory transient slip during the 2001 M_w = 8.4 Peru earthquake sequence from continuous GPS, *Geophys. Res. Lett.*, *29*(21), 2032, doi:10.1029/2002GL015533.
- Melbourne, T. I., and F. H. Webb (2003), Slow but not quite silent, *Science*, *300*, 1886–1887, doi:10.1126/science.1086163.
- Melbourne, T. I., F. H. Webb, J. M. Stock, and C. Rieger (2002), Rapid postseismic transients in subduction zones from continuous GPS, *J. Geophys. Res.*, *107*(B10), 2241, doi:10.1029/2001JB000555.
- Melbourne, T. I., W. M. Szeliga, M. M. Miller, and V. M. Santillan (2005), Extent and duration of the 2003 Cascadia slow earthquake, *Geophys. Res. Lett.*, *32*, L04301, doi:10.1029/2004GL021790.
- Miller, M. M., T. Melbourne, D. J. Johnson, and W. Q. Sumner (2002), Periodic slow earthquakes from the Cascadia subduction zone, *Science*, *295*, 2423, doi:10.1126/science.1071193.
- Miyazaki, S., J. J. McGuire, and P. Segall (2003), A transient subduction zone slip episode in southwest Japan observed by the nationwide GPS array, *J. Geophys. Res.*, *108*(B2), 2087, doi:10.1029/2001JB000456.
- Miyazaki, S., P. Segall, J. J. McGuire, T. Kato, and Y. Hatanaka (2006), Spatial and temporal evolution of stress and slip rate during the 2000 Tokai slow earthquake, *J. Geophys. Res.*, *111*, B03409, doi:10.1029/2004JB003426.
- Miyazawa, M., and J. Mori (2005), Detection of triggered deep low-frequency events from the 2003 Tokachi-oki earthquake, *Geophys. Res. Lett.*, *32*, L10307, doi:10.1029/2005GL022539.
- Miyazawa, M., and J. Mori (2006), Evidence suggesting fluid flow beneath Japan due to periodic seismic triggering from the 2004 Sumatra-Andaman earthquake, *Geophys. Res. Lett.*, *33*, L05303, doi:10.1029/2005GL025087.
- Murray, J. R., and P. Segall (2005), Spatiotemporal evolution of a transient slip event on the San Andreas Fault near Parkfield, California, *J. Geophys. Res.*, *110*, B09407, doi:10.1029/2005JB003651.
- Nadeau, R., and D. Dolenc (2005), Nonvolcanic tremors deep beneath the San Andreas Fault, *Science*, *307*, 389, doi:10.1126/science.1107142.
- Nadeau, R., and L. R. Johnson (1998), Seismological studies at Parkfield VI: Moment release rates and estimates of source parameters for small repeating earthquakes, *Bull. Seismol. Soc. Am.*, *88*, 790–814.
- Nadeau, R. M., and T. V. McEvilly (1999), Fault slip rates at depth from recurrence intervals of repeating microearthquakes, *Science*, *285*, 718–721.
- Newman, A. V., and E. A. Okal (1998), Teleseismic estimates of radiated seismic energy: The E/M_0 discriminant for tsunami earthquakes, *J. Geophys. Res.*, *103*, 26,885–26,898.
- Norabuena, E., et al. (2004), Geodetic and seismic constraints on some seismogenic zone processes in Costa Rica, *J. Geophys. Res.*, *109*, B11403, doi:10.1029/2003JB002931.
- Obara, K. (2002), Nonvolcanic deep tremor associated with subduction in southwest Japan, *Science*, *296*, 1679–1681.
- Obara, K., and H. Hirose (2006), Non-volcanic deep low-frequency tremors accompanying slow slips in the southwest Japan subduction zone, *Tectonophysics*, *417*, 33–51.
- Obara, K., H. Hirose, F. Yamamizu, and K. Kasahara (2004), Episodic slow slip events accompanied by non-volcanic tremors in southwest Japan subduction zone, *Geophys. Res. Lett.*, *31*, L23602, doi:10.1029/2004GL020848.
- Ohta, Y., F. Kimata, and T. Sagiya (2004), Reexamination of the interplate coupling in the Tokai region, central Japan, based on the GPS data in 1997–2002, *Geophys. Res. Lett.*, *31*, L24604, doi:10.1029/2004GL021404.
- Ohta, Y., J. T. Freymueller, S. Hreinsdóttir, and H. Suito (2006), A large slow slip event and the depth of the seismogenic zone in the

- south central Alaska subduction zone, *Earth Planet Sci. Lett.*, 247, 108–116.
- Okada, Y. (1985), Surface deformation due to shear and tensile faults in a half-space, *Bull. Seismol. Soc. Am.*, 75, 1135–1154.
- Ozawa, S., M. Murakami, and T. Tada (2001), Time-dependent inversion study of the slow thrust event in the Nankai Trough subduction zone, southwestern Japan, *J. Geophys. Res.*, 106, 787–802.
- Ozawa, S., M. Murakami, M. Kaidzu, T. Tada, Y. Hatanaka, H. Yarai, and T. Nishimura (2002), Detection and monitoring of ongoing aseismic slip in the Tokai region, central Japan, *Science*, 298, 1009–1012.
- Ozawa, S., S. Miyazaki, Y. Hatanaka, T. Imakiire, M. Kaidzu, and M. Murakami (2003), Characteristic silent earthquakes in the eastern part of the Boso Peninsula, central Japan, *Geophys. Res. Lett.*, 30(6), 1283, doi:10.1029/2002GL016665.
- Ozawa, S., Y. Hatanaka, M. Kaidzu, M. Murakami, T. Imakiire, and Y. Ishigaki (2004), Aseismic slip and low-frequency earthquakes in the Bungo Channel, southwestern Japan, *Geophys. Res. Lett.*, 31, L07609, doi:10.1029/2003GL019381.
- Ozawa, S., M. Murakami, K. Masaru, and H. Yuki (2005), Transient crustal deformation in Tokai region, central Japan until May 2004, *Earth Planets Space*, 57, 909–915.
- Pelayo, A. M., and D. A. Wiens (1992), Tsunami earthquakes: Slow thrust-faulting events in the accretionary wedge, *J. Geophys. Res.*, 97, 15,321–15,337.
- Pérez-Campos, X., J. J. McGuire, and G. C. Beroza (2003), Resolution of the slow earthquake/high apparent stress paradox for oceanic transform fault earthquakes, *J. Geophys. Res.*, 108(B9), 2444, doi:10.1029/2002JB002312.
- Perfettini, H., and J. Schmittbuhl (2001), Periodic loading on a creeping fault: Implications for tides, *Geophys. Res. Lett.*, 28, 435–438.
- Peterson, C., D. Christensen, and S. McNutt (2005), Episodic tremor in the Alaska/Aleutian subduction zone, *Eos Trans. AGU*, 85(47), Fall Meet. Suppl., Abstract G51B-0830.
- Pollitz, F. F., and M. J. S. Johnston (2006), Direct test of static stress versus dynamic stress triggering of aftershocks, *Geophys. Res. Lett.*, 33, L15318, doi:10.1029/2006GL026764.
- Pratt, T. L. (2006), Do episodic tremor and slip (ETS) events affect seismicity in the northern Cascadia subduction zone?, *Eos Trans. AGU*, 87(52), Fall Meet. Suppl., Abstract T54A-04.
- Prejan, S. G., D. P. Hill, E. E. Brodsky, S. E. Hough, M. J. S. Johnston, S. D. Malone, D. H. Oppenheimer, A. M. Pitt, and K. B. Richards-Dinger (2004), Remotely triggered seismicity on the United States west coast following the M_w 7.9 Denali Fault earthquake, *Bull. Seismol. Soc. Am.*, 94, 348–359.
- Pritchard, M. E., and M. Simons (2006), An aseismic slip pulse in northern Chile and along-strike variations in seismogenic behavior, *J. Geophys. Res.*, 111, B08405, doi:10.1029/2006JB004258.
- Protti, M., F. Guendel, and E. Malavassi (2001), *Evaluación del Potencial Sísmico de la Península de Nicoya*, 1st ed., 144 pp., Ed. Fundación UNA, Heredia, Costa Rica.
- Protti, M., V. Gonzales, T. Kato, T. Inuma, S. Miyasaki, K. Obana, Y. Kaneda, P. LaFemina, T. Dixon, and S. Schwartz (2004), A creep event on the shallow interface of the Nicoya Peninsula, Costa Rica seismogenic zone, *Eos Trans. AGU*, 85(47), Fall Meet. Suppl., Abstract S441D-07.
- Roeloffs, E. A. (2006), Evidence for aseismic deformation rate changes prior to earthquakes, *Annu. Rev. Earth Planet. Sci.*, 34, 591–627.
- Rogers, G., and H. Dragert (2003), Episodic tremor and slip on the Cascadia subduction zone: The chatter of silent slip, *Science*, 300, 1942–1943.
- Rokosky, J. M., S. Y. Schwartz, and K. Obara (2006), Characteristics of subduction zone tremor in SW Japan, *Eos Trans. AGU*, 87(52), Fall Meet. Suppl., Abstract V41A-1699.
- Royle, G. T., A. J. Calvert, and H. Kao (2006), Observations of non-volcanic tremor during the northern Cascadia slow-slip event in February 2002, *Geophys. Res. Lett.*, 33, L18313, doi:10.1029/2006GL027316.
- Sacks, I. S., A. T. Linde, J. A. Snoke, and S. Suyehiro (1981), A slow earthquake sequence following the Izu-Oshima earthquake of 1978, in *Earthquake Prediction: An International Review, Maurice Ewing Ser.*, vol. 4, edited by D. W. Simpson and P. G. Richards, 617–628, pp., AGU, Washington, D. C.
- Sagiya, T. (2004), Interplate coupling in the Kanto District, central Japan, and the Boso Peninsula silent earthquake in May 1996, *Pure Appl. Geophys.*, 161, 2327–2342.
- Sagiya, T., and W. Thatcher (1999), Coseismic slip resolution along a plate boundary megathrust: The Nankai Trough, southwest Japan, *J. Geophys. Res.*, 104, 1111–1130.
- Sagiya, T., A. Yoshimura, E. Iwata, K. Abe, I. Kimura, K. Uemura, and T. Takashi (1995), Establishment of permanent GPS observation network and crustal deformation monitoring in the southern Kanto and Tokai areas, *Bull. Geogr. Surv. Inst.*, 41, 105–118.
- Sassa, K. (1935), Geophysical studies on the volcano Aso. Part 1: Volcanic micro-tremors and eruptive-earthquakes, *Mem. Coll. Sci. Univ. Kyoto*, 18, 255–293.
- Satake, K., K. Wang, and B. F. Atwater (2003), Fault slip and seismic moment of the 1700 Cascadia earthquake inferred from Japanese tsunami descriptions, *J. Geophys. Res.*, 108(B11), 2535, doi:10.1029/2003JB002521.
- Sato, H., et al. (2005), Earthquake source fault beneath Tokyo, *Science*, 309, 462–464.
- Sato, T., K. Imanishi, N. Kato, and T. Sagiya (2004), Detection of a slow slip event from small signal in GPS data, *Geophys. Res. Lett.*, 31, L05606, doi:10.1029/2004GL019514.
- Schmidt, D. (2006), The 2005 Cascadia ETS event inferred from PBO tensor strainmeters and GPS, *Eos Trans. AGU*, 87(52), Fall Meet. Suppl., Abstract T41A-1545.
- Segall, P., E. K. Desmarais, D. Shelly, A. Miklius, and P. Cervelli (2006), Earthquakes triggered by silent slip events on Kilauea volcano, Hawaii, *Nature*, 444, 71–74.
- Seno, T., and T. Yamasaki (2003), Low-frequency tremors, intraslab and interplate earthquakes in southwest Japan—From a viewpoint of slab dehydration, *Geophys. Res. Lett.*, 30(22), 2171, doi:10.1029/2003GL018349.
- Shelly, D. R., G. C. Beroza, S. Ide, and S. Nakamura (2006), Low-frequency earthquakes in Shikoku, Japan and their relationship to episodic tremor and slip, *Nature*, 442, 188–191.
- Shelly, D. R., G. C. Beroza, and S. Ide (2007), Non-volcanic tremor and low-frequency earthquake swarms, *Nature*, 446, 305–307, doi:10.1038/nature05666.
- Shen, Z., Q. Wang, R. Bürgmann, Y. Wan, and J. Ning (2005), Pole-tide modulation of slow slip events at circum-Pacific subduction zones, *Bull. Seismol. Soc. Am.*, 95, 2009–2015.
- Shibazaki, B., and Y. Iio (2003), On the physical mechanism of silent slip events along the deeper part of the seismogenic zone, *Geophys. Res. Lett.*, 30(9), 1489, doi:10.1029/2003GL017047.
- Simpson, R. W., J. J. Lienkaemper, and J. S. Galehouse (2001), Variations in creep rate along the Hayward Fault, California, interpreted as changes in depth of creep, *Geophys. Res. Lett.*, 28, 2269–2272.
- Smith, S. W., and M. Wyss (1968), Displacement on the San Andreas Fault subsequent to the 1966 Parkfield earthquake, *Bull. Seismol. Soc. Am.*, 58, 1955–1973.
- Subarya, C., M. Chlieh, L. Prawirodirdjo, J.-P. Avouac, Y. Bock, K. Sieh, A. J. Meltzner, D. H. Natawidjaja, and R. McCaffrey (2006), Plate-boundary deformation associated with the great Sumatra-Andaman earthquake, *Nature*, 440, 46–51.
- Suwa, Y., S. Miura, A. Hasegawa, T. Sato, and K. Tachibana (2006), Interplate coupling beneath NE Japan inferred from three-dimensional displacement field, *J. Geophys. Res.*, 111, B04402, doi:10.1029/2004JB003203.
- Sylvester, A. G. (1993), Investigation of nearfield postseismic slip following the M_w 7.3 Landers earthquake sequence of 28 June 1992, California, *Geophys. Res. Lett.*, 20, 1079–1082.

- Szeliga, W., T. Melbourne, M. Miller, and V. Santillan (2004), Southern Cascadia episodic slow earthquakes, *Geophys. Res. Lett.*, *31*, L16602, doi:10.1029/2004GL020824.
- Tanioka, Y., and K. Satake (2001), Coseismic slip distribution of the 1946 Nankai earthquake and aseismic slips caused by the earthquake, *Earth Planets Space*, *53*, 235–241.
- Uchida, N., T. Matsuzawa, A. Hasegawa, and T. Igarashi (2003), Interplate quasi-static slip off Sanriku, NE Japan, estimated from repeating earthquakes, *Geophys. Res. Lett.*, *30*(15), 1801, doi:10.1029/2003GL017452.
- Ueda, H., M. Ohtake, and H. Sato (2001), Afterslip of the plate interface following the 1978 Miyagi-Oki Japan earthquake, as revealed from geodetic measurement data, *Tectonophysics*, *338*, 45–57.
- Vigny, C., et al. (2006), Insight into the 2004 Sumatra-Andaman earthquake from GPS measurements in southeast Asia, *Nature*, *436*, 201–206.
- Wald, D. J., and T. H. Heaton (1994), Spatial and temporal distribution of slip for the 1992 Landers, California, earthquake, *Bull. Seismol. Soc. Am.*, *84*, 668–691.
- Wald, D. J., and P. G. Somerville (1995), Variable slip rupture model for the great 1923 Kanto, Japan earthquake: Geodetic and body waveform analysis, *Bull. Seismol. Soc. Am.*, *85*, 159–177.
- Wallace, L. M., and J. Beavan (2006), A large slow slip event on the central Hikurangi subduction interface beneath the Manawatu region, North Island, New Zealand, *Geophys. Res. Lett.*, *33*, L11301, doi:10.1029/2006GL026009.
- Wallace, L. M., J. Beavan, R. McCaffrey, and D. Darby (2004), Subduction zone coupling and tectonic block rotations in the North Island, New Zealand, *J. Geophys. Res.*, *109*, B12406, doi:10.1029/2004JB003241.
- Wang, K., R. Wells, S. Mazzotti, R. D. Hyndman, and T. Sagiya (2003), A revised dislocation model of interseismic deformation of the Cascadia subduction zone, *J. Geophys. Res.*, *108*(B1), 2026, doi:10.1029/2001JB001227.
- Wesson, R. L. (1988), Dynamics of fault creep, *J. Geophys. Res.*, *93*, 8929–8951.
- Williams, P. L., and H. W. Magistrale (1989), Slip along the Superstition Hills Fault associated with the 24 November 1987 Superstition Hills, California, earthquake, *Bull. Seismol. Soc. Am.*, *79*, 390–410.
- Yagi, Y., M. Kikuchi, and T. Nishimura (2003), Co-seismic slip, post-seismic slip, and largest aftershock associated with the 1994 Sanriku-haruka-oki, Japan, earthquake, *Geophys. Res. Lett.*, *30*(22), 2177, doi:10.1029/2003GL018189.
- Yamamoto, E., S. Matsumura, and T. Ohkubo (2005), A slow slip event in the Tokai area detected by tilt and seismic observation and its possible recurrence, *Earth Planets Space*, *57*, 917–923.
- Yamanaka, Y., and M. Kikuchi (2003), Source process of the recurrent Tokachi-oki earthquake on September 26, 2003, inferred from teleseismic body waves, *Earth Planets Space*, *55*, 21–24.
- Yamanaka, Y., and M. Kikuchi (2004), Asperity map along the subduction zone in northeastern Japan inferred from regional seismic data, *J. Geophys. Res.*, *109*, B07307, doi:10.1029/2003JB002683.
- Yoshida, A., K. Hosono, T. Tsukakoshi, A. Kobayashi, H. Takayama, and S. Wiemer (2006), Change in seismic activity in the Tokai region related to weakening and strengthening of the interplate coupling, *Tectonophysics*, *417*, 17–31.
- Yoshida, S., and N. Kato (2003), Episodic aseismic slip in a two-degree-of-freedom block-spring model, *Geophys. Res. Lett.*, *30*(13), 1681, doi:10.1029/2003GL017439.

J. M. Rokosky and S. Y. Schwartz, Department of Earth and Planetary Sciences, University of California, Santa Cruz, CA 95064, USA. (susan@pmc.ucsc.edu)